materials

MDPI

Article

Highly Luminescent 4*H*-1,2,4-Triazole Derivatives: Synthesis, Molecular Structure and Photophysical Properties

Monika Olesiejuk [1,*], Agnieszka Kudelko [1] and Marcin Świątkowski [2]

[1] Department of Chemical Organic Technology and Petrochemistry, The Silesian University of Technology, Krzywoustego 4, PL-44100 Gliwice, Poland; agnieszka.kudelko@polsl.pl

[2] Department of X-ray Crystallography and Crystal Chemistry, Institute of General and Ecological Chemistry, Lodz University of Technology, Żeromskiego 116, PL-90924 Łódź, Poland; marcin.swiatkowski@p.lodz.pl

* Correspondence: monika.olesiejuk@polsl.pl; Tel.: +48-32-237-17-29

Received: 15 November 2020; Accepted: 8 December 2020; Published: 10 December 2020

Abstract: An alternative approach to the Suzuki cross-coupling reaction is used to synthesize a series of new luminophores based on 4-alkyl-4*H*-1,2,4-triazole cores conjugated via 1,4-phenylene linker to fused-bicyclic and tricyclic aromatic, or heteroaromatic arrangements. The described methodology allows one to conduct the coupling reaction with the use of commercially available boronic acids in the presence of conventional solvents or ionic liquids and produced excellent yields. It was found that the use of ultrasounds or microwaves significantly accelerates the reaction. The obtained compounds exhibited high luminescent properties and a large quantum yield of emitted photons. The X-ray molecular structures of three highly conjugated 4*H*-1,2,4-triazole representatives are also presented.

Keywords: 1,2,4-triazole derivatives; Suzuki coupling; ionic liquids; microwaves; luminescent properties

1. Introduction

In recent decades, organic compounds containing both donor and acceptor moieties connected through π-conjugated linkages have been widely investigated due to the possibility of their application in optoelectronic devices [1–3], such as organic light-emitting diodes (OLEDs), photovoltaic cells and organic field-effect transistors (OFETs). However, a potential luminophore should contain not only an extended π-conjugated system, but also other features including the proper electron–hole transporting properties, a high external quantum efficiency, as well as thermal and chemical stabilities [4,5]. Heterocyclic arrangements with highly electronegative nitrogen atoms perfectly fit the requirements for such systems. The presence of nitrogen in the aromatic ring considerably affects the electron distribution within the molecule, and also improves the intramolecular electron transport.

1,2,4-Triazoles belong to the vast family of the five-membered heterocyclic arrangements and are especially interesting due to their high nitrogen content. This scaffold occurs in two tautomeric forms with the 1*H*-1,2,4-triazole system predominating over the 4*H*-1,2,4-triazole form [6,7]. The derivatives of 4*H*-1,2,4-triazole exhibit interesting properties and, thus, have applications in diverse fields such as optoelectronics (emission properties) [8–14], materials science (corrosion inhibition) [15–20], medicine [21–32] and agriculture [33–38] (biological properties). Due to the numerous applications, the 1,2,4-triazole core has been the subject of several recent literature reviews commenting on the synthesis of these moieties [7,39–43]. The most popular methods for the construction of trisubstituted 4*H*-1,2,4-triazole derivatives are the cyclocondensation of *N*,*N*′-dichloromethylidenehydrazine using an appropriate amine, and the cyclodehydration of *N*-acylamidrazone derivatives from a large variety

of precursors depending on the nature of their substituents [7,30,40]. An interesting alternative seems to be the use of the one-pot method in the synthesis of 4*H*-1,2,4-triazole derivatives [44–46].

One of the most effective reactions to form a C–C bond are cross-coupling reactions. Among them, the methodology using a variety of commercially available organoboron compounds is particularly interesting. The Suzuki cross-coupling reaction is typically completed with various combinations of catalysts, bases or solvents, and their mutual integration affects the efficiency and selectivity of the reaction [47–49]. Suzuki cross-coupling reaction is well utilized by chemists due to the possibility of using alternative solvents such as ionic liquids (IL), or ultrasound and microwave irradiation as accelerating factors. A combination of these two aspects, such as microwave or ultrasound-assisted reactions using IL, are necessary to improve the environmental impact of chemistry. In the case of alternative solvents, the important topic worth mentioning is the low vapor pressure of the ionic liquid, and the possibility of its regeneration and reuse, which eliminates classic volatile organic solvents. It is possible to reduce energy expenditure by heating chemical reactions using microwaves or by reducing the number of reagents applied when the ionic liquid acts as a catalyst [50–54].

In our previous work, we analyzed the derivatives of five-membered heterocyclic systems such as oxadiazole, thiadiazole, and triazole, with potential applications in optoelectronics [55–58]. We showed that 1,2,4-triazole derivatives have very good emission properties. Here, we present a synthesis proceeding in an environmentally friendly manner of more extended π-conjugated systems with triazole core hoping for their equally high quantum yields of fluorescence.

2. Materials and Methods

2.1. General Information

The melting points of all compounds were measured on a Stuart SMP3 melting point apparatus (Stuart, Staffordshire, UK). The ^{1}H-NMR and ^{13}C-NMR spectra were performed in $CDCl_3$ solution using tetramethylsilane (TMS) as the internal standard on an Agilent 400-NMR spectrometer (Agilent Technologies, Waldbronn, Germany). X-ray diffraction data were collected on the Synergy Dualflex Pilatus diffractometer (Rigaku, Tokyo, Japan) (for the detailed description of the crystal structure determination, see Supplementary Materials, Section 3). All FT-IR spectra were registered between 4000 and 650 cm^{-1} using an FT-IR Nicolet 6700 apparatus with a Smart iTR accessory (Thermo Fischer Scientific, Wesel, Germany). UV–Vis spectra were recorded on a Jasco V-660 spectrophotometer (Jasco Corporation, Tokyo, Japan) at room temperature in CH_2Cl_2 ($c = 5 \times 10^{-6}$ mol/dm^3). Fluorescence spectra were recorded at room temperature in CH_2Cl_2 ($c = 5 \times 10^{-6}$ mol/dm^3) using a Jasco F-6300 fluorescence spectrophotometer (Jasco Corporation, Tokyo, Japan). High-resolution mass spectra measurements were completed on a Waters ACQUITY UPLC/Xevo G2QT instrument (Waters Corporation, Milford, MA, USA). Thin-layer chromatography was performed on silica gel 60 F_{254} Thin-Layer Chromatography (TLC) plates (Merck KGaA, Darmstadt, Germany) using $CHCl_3$/EtOAc (5:1 *v*/*v*) as the mobile phase. All reagents from commercial sources were used without additional purification. An aqueous solution of IL: choline hydroxide solution 46 wt.% in H_2O (Choline–OH) was used throughout. Ultrasound, for sonication, was generated using an EMAG Technologies Emmi 40HC operating at a frequency 38 kHz, 230 V/50 Hz with bath dimensions of 300 mm × 155 mm × 100 mm (Emag Polska, Juszczyn, Poland). The experiments using microwave radiation were performed in a CEM Discover microwave-enhanced synthesis system (CEM Corporation, Matthews, NC, USA) equipped with a personal computer.

2.2. Synthesis of Compounds

2.2.1. The Synthesis of Suzuki Cross-Coupling Precursors

4-alkyl-3,5-bis(4-bromophenyl)-4*H*-1,2,4-triazoles (**5a–d**) was completed according to the literature procedure [58] using a four-step reaction methodology starting with commercially available 4-bromobenzoic acid (**1**) (Scheme 1).

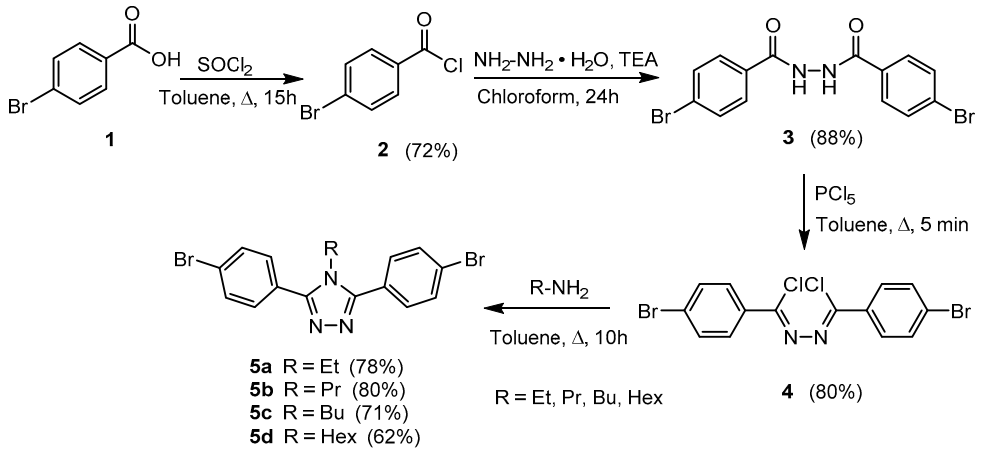

Scheme 1. Synthesis of the 4-alkyl-4*H*-1,2,4-triazole precursors.

2.2.2. A General Procedure for Conventional Suzuki Cross-Coupling Reactions

Synthesis of the 4-alkyl-3,5-bis[4′-(*N*,*N*-diphenylamino)biphenyl-4-yl]-4*H*-1,2,4-triazoles (**7–10a**).

4-Alkyl-3,5-bis(4-bromophenyl)-4*H*-1,2,4-triazole (**5a–d**, 1.00 mmol), 4-(*N*,*N*-diphenylamino) phenylboronic acid (**6a**, 2.50 mmol), palladium catalyst $Pd(PPh_3)_4$ (0.058 g, 0.05 mmol), a phase transfer catalyst NBu_4Br (0.032 g, 0.10 mmol), and base K_2CO_3 (1.382 g, 10.00 mmol) were added to a combination of toluene (9 mL), H_2O (6 mL) and EtOH (3 mL). The mixture was heated under reflux in an oil bath (130 °C) for 7 h (TLC). After cooling, the mixture was transferred to a separating funnel and chloroform (50 mL) was added. After additional extraction with chloroform (2 × 10 mL), the combined organic layers were filtered through a silica gel plug (10 mL). The silica layer was then rinsed with $CHCl_3$/EtOAc (5:1 *v*/*v*). The filtrate was dried with $MgSO_4$ and concentrated on the rotary evaporator. The product was precipitated using EtOAc (5 mL), filtered, washed with fresh EtOAc, and air-dried to give pure 4-alkyl-3,5-bis[4′-(*N*,*N*-diphenylamino)biphenyl-4-yl]-4*H*-1,2,4-triazoles (**7–10a**).

2.2.3. A General Procedure for IL Alternative Approach for Suzuki Cross-Coupling Reactions

Synthesis of the 4-alkyl-3,5-bis(4-arylphenyl)-4*H*-1,2,4-triazoles **7a–k**, **8a**, **9a–k**, **10a**.

4-Alkyl-3,5-bis(4-bromophenyl)-4*H*-1,2,4-triazole (**5a–d**, 1.00 mmol), an appropriate boronic acid (**6a–k**, 2.50 mmol), and $Pd(PPh_3)_4$ (0.058 g, 0.05 mmol) were added to a mixture of aqueous choline hydroxide solution 46 wt.% (Choline–OH, 10 mL) and toluene (1 mL). The reaction monitored by TLC was carried out using conventional heating—an oil bath (130 °C) or ultrasonication—an ultrasonic bath (80 °C), or microwave irradiation (150 W) in 3–5 cycles of 90 s with 2 min intervals at a temperature 50–100 °C. After cooling, mixture was transferred to a separating funnel and chloroform (50 mL) was added. After the additional extraction with chloroform (2 × 10 mL), the combined chloroform layers were filtered through a silica gel plug (10 mL). The silica layer was then rinsed with $CHCl_3$/EtOAc (5:1 *v*/*v*). The filtrate was dried with $MgSO_4$ and concentrated on the rotary evaporator. The product was precipitated using EtOAc (5 mL), filtered, washed with fresh EtOAc, and air-dried to give corresponding 4-alkyl-3,5-bis(4-arylphenyl)-4*H*-1,2,4-triazoles **7a–k**, **8a**, **9a–k**, **10a**.

2.3. Characterization of Compounds

4-Ethyl-3,5-bis[4′-(*N*,*N*-diphenylamino)biphenyl-4-yl]-4*H*-1,2,4-triazole (**7a**). Yellow solid in 97% yield, 0.357 g, m.p. 268–270 °C; UV (CH_2Cl_2) λ_{max} 351.0 nm ($\varepsilon \cdot 10^{-3}$ 59.5 $cm^{-1}M^{-1}$); IR (ATR) ν: 3033, 1731, 1588, 1509, 1483, 1327, 1272, 1219, 1181, 1075, 1028, 821, 772, 749, 694, 666, 621 cm^{-1}; ^{1}H-NMR (400 MHz, $CDCl_3$): δ 1.16 (t, *J* = 7.2 Hz, 3H, CH_3), 4.23 (q, *J* = 7.2 Hz, 2H, CH_2), 7.06 (t, *J* = 7.2 Hz, 4H, ArH), 7.13–7.18 (m, 12H, ArH), 7.28 (t, *J* = 7.2 Hz, 8H, ArH), 7.54 (d, *J* = 8.4 Hz, 4H, ArH), 7.71–7.75 (m, 8H, ArH); ^{13}C-NMR (100 MHz, $CDCl_3$): δ 15.8, 40.0, 123.2, 123.6, 124.6, 126.0, 126.9, 127.8, 129.3, 129.4, 133.5, 142.2, 147.5, 147.9, 155.1; HRMS *m*/*z* calcd for ($C_{52}H_{41}N_5$ + H^+): 736.3440; found: 736.3441.

4-Ethyl-3,5-bis[4-(naphthalen-1-yl)phenyl]-4*H*-1,2,4-triazole (**7b**). Beige solid in 88% yield, 0.221 g, m.p. 308–310 °C; UV (CH_2Cl_2) λ_{max} 297.0 nm ($\varepsilon \cdot 10^{-3}$ 36.4 $cm^{-1}M^{-1}$); IR (ATR) ν: 3055, 2980, 1591, 1506, 1478, 1425, 1395, 1340, 1250, 1108, 1018, 967, 951, 829, 802, 793, 780, 754, 729 cm^{-1}; ^{1}H-NMR (400 MHz, $CDCl_3$): δ 1.29 (t, *J* = 7.2 Hz, 3H, CH_3), 4.36 (q, *J* = 7.2 Hz, 2H, CH_2), 7.47–7.59 (m, 8H, ArH), 7.69 (d, *J* = 8.4 Hz, 4H, ArH), 7.86 (d, *J* = 8.4 Hz, 4H, ArH), 7.91–7.96 (m, 6H, ArH); ^{13}C-NMR (100 MHz, $CDCl_3$): δ 16.1, 40.1, 125.4, 125.7, 126.0, 126.4, 126.7, 127.0, 128.2, 128.4, 128.9, 130.7, 131.4, 133.8, 139.2, 142.7, 155.3; HRMS *m/z* calcd for ($C_{36}H_{27}N_3$ + H^+): 502.2283; found: 502.2281.

4-Ethyl-3,5-bis[4-(naphthalen-2-yl)phenyl]-4*H*-1,2,4-triazole (**7c**). White solid in 99% yield, 0.248 g, m.p. 292–295 °C; UV (CH_2Cl_2) λ_{max} 268.0 nm ($\varepsilon \cdot 10^{-3}$ 57.3 $cm^{-1}M^{-1}$) and 305.0 (45.0); IR (ATR) ν: 3051, 1473, 1423, 1401, 1360, 1211, 1080, 1017, 969, 956, 898, 857, 815, 752, 719 cm^{-1}; ^{1}H-NMR (400 MHz, $CDCl_3$): δ 1.22 (t, *J* = 7.2 Hz, 3H, CH_3), 4.29 (q, *J* = 7.2 Hz, 2H, CH_2), 7.50–7.57 (m, 4H, ArH), 7.81 (dd, *J* = 8.4 and 1.6 Hz, 2H, ArH), 7.84 (d, *J* = 8.8 Hz, 4H, ArH), 7.88–7.95 (m, 8H, ArH), 7.97 (d, *J* = 8.4 Hz, 2H, ArH), 8.13 (d, *J* = 1.6 Hz, 2H, ArH); ^{13}C-NMR (100 MHz, $CDCl_3$): δ 16.0, 40.1, 125.2, 126.1, 126.3, 126.5, 126.7, 127.7, 127.9, 128.3, 128.7, 129.4, 132.9, 133.6, 137.4, 142.8, 155.2; HRMS *m/z* calcd for ($C_{36}H_{27}N_3$ + H^+): 502.2283; found: 502.2287.

4-Ethyl-3,5-bis[4-(quinolin-3-yl)phenyl]-4*H*-1,2,4-triazole (**7d**). White solid in 79% yield, 0.198 g, m.p. 296–298 °C; UV (CH_2Cl_2) λ_{max} 269.0 nm ($\varepsilon \cdot 10^{-3}$ 52.8 $cm^{-1}M^{-1}$) and 305.0 (42.6); IR (ATR) ν: 3069, 3002, 2964, 1494, 1477, 1468, 1453, 1379, 1358, 1543, 1202, 1081, 1019, 963, 952, 931, 912, 868, 856, 841, 795, 781, 767, 761, 744, 738, 726 cm^{-1}; ^{1}H-NMR (400 MHz, $CDCl_3$): δ 1.23 (t, *J* = 7.2 Hz, 3H, CH_3), 4.30 (q, *J* = 7.2 Hz, 2H, CH_2), 7.62 (t, *J* = 8.0 Hz, 2H, ArH), 7.77 (t, *J* = 8.0 Hz, 2H, ArH), 7.88–7.94 (m, 10H, ArH), 8.18 (d, *J* = 8.0 Hz, 2H, ArH), 8.40 (d, *J* = 2.4 Hz, 2H, ArH), 9.25 (d, *J* = 2.4 Hz, 2H, ArH); ^{13}C-NMR (100 MHz, $CDCl_3$): δ 16.0, 40.1, 127.3, 127.4, 127.8, 127.9, 128.1, 129.3, 129.7, 129.8, 132.7, 133.6, 139.7, 147.7, 149.5, 155.0; HRMS *m/z* calcd for ($C_{34}H_{25}N_5$ + H^+): 504.2188; found: 504.2188.

4-Ethyl-3,5-bis[4-(quinolin-6-yl)phenyl]-4*H*-1,2,4-triazole (**7e**). Pearl solid in 94% yield, 0.236 g, m.p. 302–305 °C; UV (CH_2Cl_2) λ_{max} 269.0 nm ($\varepsilon \cdot 10^{-3}$ 56.4 $cm^{-1}M^{-1}$) and 306.0 (42.0); IR (ATR) ν: 3052, 1593, 1570, 1499, 1474, 1424, 1347, 1326, 1121, 1014, 971, 892, 868, 856, 831, 797, 781, 754 cm^{-1}; ^{1}H-NMR (400 MHz, $CDCl_3$): δ 1.22 (t, *J* = 7.2 Hz, 3H, CH_3), 4.30 (q, *J* = 7.2 Hz, 2H, CH_2), 7.47 (dd, *J* = 8.4 and 4.4 Hz, 2H, ArH), 7.85 (d, *J* = 8.4 Hz, 4H, ArH), 7.91 (d, *J* = 8.4 Hz, 4H, ArH), 8.05 (dd, *J* = 8.4 and 2.0 Hz, 2H, ArH), 8.09 (d, *J* = 2.0 Hz, 2H, ArH), 8.22–8.26 (m, 4H, ArH), 8.96 (dd, *J* = 4.4 and 2.0 Hz, 2H, ArH); ^{13}C-NMR (100 MHz, $CDCl_3$): δ 16.0, 40.1, 121.7, 125.8, 127.0, 128.0, 128.5, 128.9, 129.5, 130.2, 136.3, 138.1, 142.0, 147.9, 150.8, 155.1; HRMS *m/z* calcd for ($C_{34}H_{25}N_5$ + H^+): 504.2188; found: 504.2189.

3,5-Bis[4-(dibenzothiophen-4-yl)phenyl]-4-ethyl-4*H*-1,2,4-triazole (**7f**). Creamy solid in 96% yield, 0.296 g, m.p. 281–283 °C; UV (CH_2Cl_2) λ_{max} 240.0 nm ($\varepsilon \cdot 10^{-3}$ 85.0 $cm^{-1}M^{-1}$) and 290.0 (48.5); IR (ATR) ν: 3062, 1470, 1440, 1425, 1391, 1376, 1360, 1246, 1112, 1016, 863, 836, 800, 753, 743, 730, 718, 704 cm^{-1}; ^{1}H-NMR (400 MHz, $CDCl_3$): δ 1.28 (t, *J* = 7.2 Hz, 3H, CH_3), 4.35 (q, *J* = 7.2 Hz, 2H, CH_2), 7.48–7.51 (m, 4H, ArH), 7.56 (d, *J* = 7.6 Hz, 2H, ArH), 7.61 (t, *J* = 7.6 Hz, 2H, ArH), 7.86 (d, *J* = 7.6 Hz, 2H, ArH), 7.90 (d, *J* = 8.4 Hz, 4H, ArH), 7.95 (d, *J* = 8.4 Hz, 4H, ArH), 8.20–8.23 (m, 4H, ArH); ^{13}C-NMR (100 MHz, $CDCl_3$): δ 16.0, 40.1, 121.0, 121.8, 122.7, 124.5, 125.2, 127.0, 127.3, 128.9, 129.4, 135.7, 135.9, 136.5, 138.5, 139.4, 142.4, 152.2, 155.1; HRMS *m/z* calcd for ($C_{40}H_{27}N_3S_2$ + H^+): 614.1725; found: 614.1727.

3,5-Bis[4-(dibenzofuran-4-yl)phenyl]-4-ethyl-4*H*-1,2,4-triazole (**7g**). Creamy solid in 92% yield, 0.267 g, m.p. 255–256 °C; UV (CH_2Cl_2) λ_{max} 286.0 nm ($\varepsilon \cdot 10^{-3}$ 70.5 $cm^{-1}M^{-1}$) and 315.0 (41.0); IR (ATR) ν: 3055, 2949, 1586, 1479, 1450, 1430, 1412, 1395, 1360, 1259, 1189, 1101, 1058, 1014, 968, 874, 838, 801, 791, 741, 729 cm^{-1}; ^{1}H-NMR (400 MHz, $CDCl_3$): δ 1.27 (t, *J* = 7.2 Hz, 3H, CH_3), 4.35 (q, *J* = 7.2 Hz, 2H, CH_2), 7.39 (t, *J* = 8.0 Hz, 2H, ArH), 7.46–7.52 (m, 4H, ArH), 7.65 (d, *J* = 8.0 Hz, 2H, ArH), 7.70 (d, *J* = 8.0 Hz, 2H, ArH), 7.91 (d, *J* = 8.4 Hz, 4H, ArH), 7.99–8.03 (m, 4H, ArH), 8.14 (d, *J* = 8.4 Hz, 4H, ArH); ^{13}C-NMR (100 MHz, $CDCl_3$): δ 16.1, 40.1, 111.9, 120.3, 120.8, 123.0, 123.4, 124.1, 124.7, 125.2, 126.8, 127.0, 127.4, 129.2, 129.3, 138.2, 153.3, 155.2, 156.2; HRMS *m/z* calcd for ($C_{40}H_{27}N_3O_2$ + H^+): 582.2182; found: 582.2183.

4-Ethyl-3,5-bis[4-(9-methyl-9*H*-carbazol-3-yl)phenyl]-4*H*-1,2,4-triazole (**7h**). Creamy solid in 70% yield, 0.107 g, m.p. 313–315 °C; UV (CH_2Cl_2) λ_{max} 300.0 nm ($\varepsilon \cdot 10^{-3}$ 69.9 $cm^{-1}M^{-1}$) and 321.0 (46.0);

IR (ATR) ν: 3054, 2990, 2935, 1598, 1483, 1466, 1424, 1359, 1337, 1323, 1294, 1254, 1221, 1120, 1012, 844, 825, 804, 764, 750, 739, 719 cm^{-1}; ^{1}H-NMR (400 MHz, $CDCl_3$): δ 1.22 (t, *J* = 7.2 Hz, 3H, CH_3), 3.92 (s, 6H, CH_3), 4.29 (q, *J* = 7.2 Hz, 2H, CH_2), 7.29 (t, *J* = 7.6 Hz, 2H, ArH), 7.45 (d, *J* = 7.6 Hz, 2H, ArH), 7.50–7.55 (m, 4H, ArH), 7.80–7.83 (m, 6H, ArH), 7.91 (d, *J* = 8.4 Hz, 4H, ArH), 8.18 (d, *J* = 7.6 Hz, 2H, ArH), 8.40 (s, 2H, ArH); ^{13}C-NMR (100 MHz, $CDCl_3$): δ 15.9, 29.3, 40.0, 108.7, 108.9, 118.9, 119.2, 120.4, 122.9, 123.4, 125.1, 125.7, 126.1, 127.6, 129.4, 131.1, 140.9, 141.5, 143.8, 155.3; HRMS *m/z* calcd for ($C_{42}H_{33}N_5$ + H^+): 608.2814; found: 608.2817.

4-Ethyl-3,5-bis[4-(9-ethyl-9*H*-carbazol-3-yl)phenyl]-4*H*-1,2,4-triazole (**7i**). Creamy solid in 76% yield, 0.121 g, m.p. 232–234 °C; UV (CH_2Cl_2) λ_{max} 243.0 nm (ε·10^{-3} 54.6 $cm^{-1}M^{-1}$), 301.0 (76.5) and 322.0 (49.9); IR (ATR) ν: 3047, 2977, 1597, 1459, 1379, 1346, 1334, 1295, 1254, 1233, 1196, 1154, 1125, 1086, 848, 806, 769, 747, 729, 695 cm^{-1}; ^{1}H-NMR (400 MHz, $CDCl_3$): δ 1.22 (t, *J* = 7.2 Hz, 3H, CH_3), 1.49 (t, *J* = 7.2 Hz, 6H, CH_3), 4.29 (q, *J* = 7.2 Hz, 2H, CH_2), 4.43 (q, *J* = 7.2 Hz, 4H, CH_2), 7.28 (t, *J* = 7.6 Hz, 2H, ArH), 7.45 (d, *J* = 7.6 Hz, 2H, ArH), 7.49–7.53 (m, 4H, ArH), 7.79 (d, *J* = 7.6 Hz, 2H, ArH), 7.83 (d, *J* = 8.4 Hz, 4H, ArH), 7.90 (d, *J* = 8.4 Hz, 4H, ArH), 8.18 (d, *J* = 7.6 Hz, 2H, ArH), 8.40 (s, 2H, ArH); ^{13}C-NMR (100 MHz, $CDCl_3$): δ 13.8, 15.9, 37.7, 40.0, 108.7, 108.9, 119.0, 119.1, 120.5, 123.0, 123.6, 125.1, 125.7, 126.0, 127.6, 129.3, 131.0, 139.8, 140.5, 143.8, 155.3; HRMS *m/z* calcd for ($C_{44}H_{37}N_5$ + H^+): 636.3127; found: 636.3124.

3,5-Bis[4′-(9*H*-carbazol-9-yl)biphenyl-4-yl]-4-ethyl-4*H*-1,2,4-triazole (**7j**). Grey solid in 77% yield, 0.141 g, m.p. 277–280 °C; UV (CH_2Cl_2) λ_{max} 293.0 nm (ε·10^{-3} 50.0 $cm^{-1}M^{-1}$) and 322.0 (41.7); IR (ATR) ν: 3055, 1740, 1599, 1521, 1477, 1450, 1414, 1367, 1334, 1318, 1303, 1227, 1184, 1170, 1119, 1004, 969, 825, 742, 719 cm^{-1}; ^{1}H-NMR (400 MHz, $CDCl_3$): δ 1.25 (t, *J* = 7.2 Hz, 3H, CH_3), 4.32 (q, *J* = 7.2 Hz, 2H, CH_2), 7.32 (t, *J* = 7.6 Hz, 4H, ArH), 7.45 (t, *J* = 7.6 Hz, 4H, ArH), 7.51 (d, *J* = 7.6 Hz, 4H, ArH), 7.72 (d, *J* = 8.4 Hz, 4H, ArH), 7.86–7.92 (m, 12H, ArH), 8.19 (d, *J* = 7.6 Hz, 4H, ArH); ^{13}C-NMR (100 MHz, $CDCl_3$): δ 16.0, 40.1, 109.8, 120.1, 120.4, 123.5, 126.0, 126.9, 127.5, 127.6, 128.6, 129.5, 137.6, 139.0, 140.8, 142.0, 155.1; HRMS *m/z* calcd for ($C_{52}H_{37}N_5$ + H^+): 732.3127; found: 732.3126.

4-Ethyl-3,5-bis[4-(thiantren-1-yl)phenyl]-4*H*-1,2,4-triazole (**7k**). Grey solid in 87% yield, 0.585 g, m.p. 198–200 °C; UV (CH_2Cl_2) λ_{max} 263.0 nm (ε·10^{-3} 53.9 $cm^{-1}M^{-1}$); IR (ATR) ν: 3051, 1475, 1441, 1425, 1396, 1190, 1107, 1017, 967, 853, 842, 787, 748, 728, 686, 664, 653, 604 cm^{-1}; ^{1}H-NMR (400 MHz, $CDCl_3$): δ 1.30 (t, *J* = 7.2 Hz, 3H, CH_3), 4.35 (q, *J* = 7.2 Hz, 2H, CH_2), 7.20 (t, *J* = 7.6 Hz, 2H, ArH), 7.26 (t, *J* = 7.6 Hz, 2H, ArH), 7.30–7.36 (m, 4H, ArH), 7.39 (d, *J* = 7.6 Hz, 2H, ArH), 7.51 (d, *J* = 7.6 Hz, 2H, ArH), 7.57 (d, *J* = 7.6 Hz, 2H, ArH), 7.60 (d, *J* = 8.4 Hz, 4H, ArH), 7.84 (d, *J* = 8.4 Hz, 4H, ArH); ^{13}C-NMR (100 MHz, $CDCl_3$): δ 16.0, 40.1, 127.2, 127.7, 127.9, 128.3, 128.6, 128.6, 128.7, 128.9, 129.1, 130.1, 135.0, 135.6, 135.9, 136.2, 141.5, 142.0, 155.2; HRMS *m/z* calcd for ($C_{40}H_{27}N_3S_4$ + H^+): 678.1166; found: 678.1166.

3,5-Bis[4′-(*N*,*N*-diphenylamino)biphenyl-4-yl]-4-propyl-4*H*-1,2,4-triazole (**8a**). Yellow solid in 93% yield, 0.347 g, m.p. 189–192 °C; UV (CH_2Cl_2) λ_{max} 352.0 nm (ε·10^{-3} 51.8 $cm^{-1}M^{-1}$); IR (ATR) ν: 3033, 2958, 1735, 1587, 1509, 1486, 1327, 1272, 1241, 1179, 1046, 1004, 862, 843, 819, 773, 753, 737, 693 cm^{-1}; ^{1}H-NMR (400 MHz, $CDCl_3$): δ 0.66 (t, *J* = 7.2 Hz, 3H, CH_3), 1.49 (sext, *J* = 7.2 Hz, 2H, CH_2), 4.13 (t, *J* = 7.2 Hz, 2H, CH_2), 7.06 (t, *J* = 7.2 Hz, 4H, ArH), 7.14–7.18 (m, 12H, ArH), 7.28 (t, *J* = 7.2 Hz, 8H, ArH), 7.55 (d, *J* = 8.4 Hz, 4H, ArH), 7.71–7.75 (m, 8H, ArH); ^{13}C-NMR (100 MHz, $CDCl_3$): δ 10.7, 23.4, 46.6, 123.2, 123.6, 124.6, 126.1, 126.9, 127.7, 129.3, 129.4, 133.5, 142.1, 147.5, 147.8, 155.5; HRMS *m/z* calcd for ($C_{53}H_{43}N_5$ + H^+): 750.3597; found: 750.3588.

4-Butyl-3,5-bis[4′-(*N*,*N*-diphenylamino)biphenyl-4-yl]-4*H*-1,2,4-triazole (**9a**). Creamy solid in 99% yield, 0.382 g, m.p. 208–209 °C; UV (CH_2Cl_2) λ_{max} 351.0 nm (ε·10^{-3} 52.5 $cm^{-1}M^{-1}$); IR (ATR) ν: 3034, 2959, 2864, 1735, 1586, 1487, 1326, 1273, 1239, 1178, 1046, 1004, 974, 861, 843, 821, 754, 737, 693 cm^{-1}; ^{1}H-NMR (400 MHz, $CDCl_3$): δ 0.68 (t, *J* = 7.6 Hz, 3H, CH_3), 1.06 (sext, *J* = 7.6 Hz, 2H, CH_2), 1.43 (quin, *J* = 7.6 Hz, 2H, CH_2), 4.17 (t, *J* = 7.6 Hz, 2H, CH_2), 7.06 (t, *J* = 7.2 Hz, 4H, ArH), 7.14–7.18 (m, 12H, ArH), 7.29 (t, *J* = 7.2 Hz, 8H, ArH), 7.54 (d, *J* = 8.4 Hz, 4H, ArH), 7.71–7.75 (m, 8H, ArH); ^{13}C-NMR (100 MHz, $CDCl_3$): δ 13.2, 19.3, 32.0, 44.8, 123.2, 123.6, 124.6, 126.1, 126.9, 127.7, 129.3, 129.4, 133.5, 142.1, 147.5, 147.9, 155.4; HRMS *m/z* calcd for ($C_{54}H_{45}N_5$ + H^+): 764.3753; found: 764.3749.

4-Butyl-3,5-bis[4-(naphthalen-1-yl)phenyl]-4*H*-1,2,4-triazole (**9b**). Grey solid in 62% yield, 0.165 g, m.p. 217–218 °C; UV (CH_2Cl_2) λ_{max} 296.0 nm ($\varepsilon \cdot 10^{-3}$ 40.6 $cm^{-1}M^{-1}$); IR (ATR) ν: 3058, 2928, 2869, 1472, 1429, 1393, 1336, 1183, 1020, 965, 952, 858, 845, 831, 799, 791, 774, 752, 724 cm^{-1}; ^{1}H-NMR (400 MHz, $CDCl_3$): δ 0.77 (t, *J* = 7.6 Hz, 3H, CH_3), 1.17 (sext, *J* = 7.6 Hz, 2H, CH_2), 1.57 (quin, *J* = 7.6 Hz, 2H, CH_2), 4.30 (t, *J* = 7.6 Hz, 2H, CH_2), 7.47–7.59 (m, 8H, ArH), 7.69 (d, *J* = 8.4 Hz, 4H, ArH), 7.86 (d, *J* = 8.4 Hz, 4H, ArH), 7.90–7.96 (m, 6H, ArH); ^{13}C-NMR (100 MHz, $CDCl_3$): δ 13.3, 19.4, 32.2, 44.8, 125.4, 125.7, 126.0, 126.4, 126.8, 127.0, 128.2, 128.4, 128.9, 130.7, 131.4, 133.8, 139.2, 142.7, 155.5; HRMS *m/z* calcd for ($C_{38}H_{31}N_3$ + H^+): 530.2596; found: 530.2596.

4-Butyl-3,5-bis[4-(naphthalen-2-yl)phenyl]-4*H*-1,2,4-triazole (**9c**). Creamy solid in 89% yield, 0.236 g, m.p. 331–334 °C; UV (CH_2Cl_2) λ_{max} 269.0 nm ($\varepsilon \cdot 10^{-3}$ 73.8 $cm^{-1}M^{-1}$) and 305.0 (58.9); IR (ATR) ν: 3050, 2954, 2872, 1597, 1489, 1465, 1402, 1368, 1211, 1016, 972, 951, 895, 841, 813, 751, 717 cm^{-1}; ^{1}H-NMR (400 MHz, $CDCl_3$): δ 0.72 (t, *J* = 7.6 Hz, 3H, CH_3), 1.10 (sext, *J* = 7.6 Hz, 2H, CH_2), 1.50 (quin, *J* = 7.6 Hz, 2H, CH_2), 4.24 (t, *J* = 7.6 Hz, 2H, CH_2), 7.51–7.57 (m, 4H, ArH), 7.81–7.85 (m, 6H, ArH), 7.89–7.95 (m, 8H, ArH), 7.97 (d, *J* = 8.8 Hz, 2H, ArH), 8.14 (d, *J* = 1.2 Hz, 2H, ArH); ^{13}C-NMR (100 MHz, $CDCl_3$): δ 13.3, 19.4, 32.1, 44.9, 125.2, 126.1, 126.3, 126.5, 126.8, 127.7, 127.9, 128.3, 128.7, 129.4, 132.9, 133.6, 137.4, 142.7, 155.4; HRMS *m/z* calcd for ($C_{38}H_{31}N_3$ + H^+): 530.2596; found: 530.2598.

4-Butyl-3,5-bis[4-(quinolin-3-yl)phenyl]-4*H*-1,2,4-triazole (**9d**). Grey solid in 99% yield, 0.263 g, m.p. 310–313 °C; UV (CH_2Cl_2) λ_{max} 270.0 nm ($\varepsilon \cdot 10^{-3}$ 37.5 $cm^{-1}M^{-1}$) and 304.0 (30.4); IR (ATR) ν: 3060, 2961, 2918, 2862, 1574, 1489, 1471, 1436, 1363, 1208, 1018, 972, 951, 906, 861, 844, 833, 783, 745, 724 cm^{-1}; ^{1}H-NMR (400 MHz, $CDCl_3$): δ 0.73 (t, *J* = 7.6 Hz, 3H, CH_3), 1.11 (sext, *J* = 7.6 Hz, 2H, CH_2), 1.50 (quin, *J* = 7.6 Hz, 2H, CH_2), 4.26 (t, *J* = 7.6 Hz, 2H, CH_2), 7.63 (t, *J* = 8.0 Hz, 2H, ArH), 7.77 (t, *J* = 8.0 Hz, 2H, ArH), 7.88–7.95 (m, 10H, ArH), 8.18 (d, *J* = 8.0 Hz, 2H, ArH), 8.41 (d, *J* = 2.4 Hz, 2H, ArH), 9.26 (d, *J* = 2.4 Hz, 2H, ArH); ^{13}C-NMR (100 MHz, $CDCl_3$): δ 13.3, 19.4, 32.2, 45.0, 127.3, 127.5, 127.8, 127.9, 128.1, 129.3, 129.7, 129.8, 132.7, 133.6, 139.6, 147.7, 149.5, 155.3; HRMS *m/z* calcd for ($C_{36}H_{29}N_5$ + H^+): 532.2501; found: 532.2507.

4-Butyl-3,5-bis[4-(quinolin-6-yl)phenyl]-4*H*-1,2,4-triazole (**9e**). White solid in 91% yield, 0.242 g, m.p. 268–270 °C; UV (CH_2Cl_2) λ_{max} 271.0 nm ($\varepsilon \cdot 10^{-3}$ 52.9 $cm^{-1}M^{-1}$) and 306.0 (39.8); IR (ATR) ν: 2954, 2872, 1593, 1571, 1481, 1351, 1127, 975, 886, 870, 827, 792, 776, 743, 716 cm^{-1}; ^{1}H-NMR (400 MHz, $CDCl_3$): δ 0.72 (t, *J* = 7.6 Hz, 3H, CH_3), 1.11 (sext, *J* = 7.6 Hz, 2H, CH_2), 1.50 (quin, *J* = 7.6 Hz, 2H, CH_2), 4.25 (t, *J* = 7.6 Hz, 2H, CH_2), 7.47 (dd, *J* = 8.4 and 4.4 Hz, 2H, ArH), 7.86 (d, *J* = 8.4 Hz, 4H, ArH), 7.92 (d, *J* = 8.4 Hz, 4H, ArH), 8.05 (dd, *J* = 8.4 and 2.0 Hz, 2H, ArH), 8.10 (d, *J* = 2.0 Hz, 2H, ArH), 8.22–8.27 (m, 4H, ArH), 8.96 (dd, *J* = 4.4 and 2.0 Hz, 2H, ArH); ^{13}C-NMR (100 MHz, $CDCl_3$): δ 13.3, 19.4, 32.1, 44.9, 121.7, 125.8, 127.2, 127.9, 128.5, 128.9, 129.5, 130.2, 136.3, 138.1, 141.9, 147.9, 150.8, 155.4; HRMS *m/z* calcd for ($C_{36}H_{29}N_5$ + H^+): 532.2501; found: 532.2504.

3,5-Bis[4-(dibenzothiophen-4-yl)phenyl]-4-butyl-4*H*-1,2,4-triazole (**9f**). Creamy solid in 93% yield, 0.299 g, m.p. 256–258 °C; UV (CH_2Cl_2) λ_{max} 241.0 nm ($\varepsilon \cdot 10^{-3}$ 40.5 $cm^{-1}M^{-1}$) and 290.0 (22.4); IR (ATR) ν: 3056, 2959, 1472, 1441, 1377, 1249, 1101, 1048, 1020, 973, 846, 826, 804, 796, 755, 742, 727, 704 cm^{-1}; ^{1}H-NMR (400 MHz, $CDCl_3$): δ 0.76 (t, *J* = 7.6 Hz, 3H, CH_3), 1.16 (sext, *J* = 7.6 Hz, 2H, CH_2), 1.55 (quin, *J* = 7.6 Hz, 2H, CH_2), 4.29 (t, *J* = 7.6 Hz, 2H, CH_2), 7.48–7.51 (m, 4H, ArH), 7.56 (d, *J* = 7.6 Hz, 2H, ArH), 7.61 (t, *J* = 7.6 Hz, 2H, ArH), 7.86 (d, *J* = 7.6 Hz, 2H, ArH), 7.89 (d, *J* = 8.4 Hz, 4H, ArH), 7.95 (d, *J* = 8.4 Hz, 4H, ArH), 8.20–8.23 (m, 4H, ArH); ^{13}C-NMR (100 MHz, $CDCl_3$): δ 13.3, 19.4, 32.2, 44.9, 121.0, 121.8, 122.7, 124.5, 125.2, 127.0, 127.4, 128.9, 129.4, 135.7, 135.9, 136.5, 138.5, 139.4, 142.4, 152.2, 155.4; HRMS *m/z* calcd for ($C_{42}H_{31}N_3S_2$ + H^+): 642.2038; found: 642.2034.

3,5-Bis[4-(dibenzofuran-4-yl)phenyl]-4-butyl-4*H*-1,2,4-triazole (**9g**). Creamy solid in 88% yield, 0.268 g, m.p. 228–230 °C; UV (CH_2Cl_2) λ_{max} 286.0 nm ($\varepsilon \cdot 10^{-3}$ 57.0 $cm^{-1}M^{-1}$) and 317.0 (30.6); IR (ATR) ν: 3049, 2960, 1737, 1471, 1450, 1430, 1411, 1386, 1237, 1220, 1192, 1174, 1063, 1014, 975, 854, 841, 812, 792, 772, 741 cm^{-1}; ^{1}H-NMR (400 MHz, $CDCl_3$): δ 0.75 (t, *J* = 7.6 Hz, 3H, CH_3), 1.15 (sext, *J* = 7.6 Hz, 2H, CH_2), 1.55 (quin, *J* = 7.6 Hz, 2H, CH_2), 4.30 (t, *J* = 7.6 Hz, 2H, CH_2), 7.39 (t, *J* = 8.0 Hz, 2H, ArH), 7.46–7.53 (m, 4H, ArH), 7.65 (d, *J* = 8.0 Hz, 2H, ArH), 7.71 (d, *J* = 8.0 Hz, 2H, ArH), 7.91 (d, *J* = 8.4 Hz, 4H, ArH), 7.99–8.03 (m, 4H, ArH), 8.14 (d, *J* = 8.4 Hz, 4H, ArH); ^{13}C-NMR (100 MHz, $CDCl_3$): δ 13.3,

19.4, 32.2, 45.0, 111.9, 120.3, 120.8, 122.9, 123.3, 124.1, 124.7, 125.2, 126.8, 127.1, 127.4, 129.2, 129.3, 138.1, 153.4, 155.5, 156.2; HRMS *m/z* calcd for ($C_{42}H_{31}N_3O_2$ + H^+): 610.2495; found: 610.2491.

4-Butyl-3,5-bis[4-(9-methyl-9*H*-carbazol-3-yl)phenyl]-4*H*-1,2,4-triazole (**9h**). Creamy solid in 97% yield, 0.308 g, m.p. 267–268 °C; UV (CH_2Cl_2) λ_{max} 300.0 nm ($\varepsilon \cdot 10^{-3}$ 76.8 $cm^{-1}M^{-1}$) and 323.0 (51.0); IR (ATR) ν: 3047, 2957, 2934, 1597, 1483, 1466, 1424, 1360, 1335, 1323, 1294, 1254, 1221, 1154, 1121, 1012, 843, 825, 813, 799, 772, 749, 739, 721 cm^{-1}; ^{1}H-NMR (400 MHz, $CDCl_3$): δ 0.73 (t, *J* = 7.6 Hz, 3H, CH_3), 1.11 (sext, *J* = 7.6 Hz, 2H, CH_2), 1.50 (quin, *J* = 7.6 Hz, 2H, CH_2), 3.91 (s, 6H, CH_3), 4.24 (t, *J* = 7.6 Hz, 2H, CH_2), 7.28 (t, *J* = 7.6 Hz, 2H, ArH), 7.44 (d, *J* = 7.6 Hz, 2H, ArH), 7.49–7.54 (m, 4H, ArH), 7.80–7.82 (m, 6H, ArH), 7.90 (d, *J* = 8.4 Hz, 4H, ArH), 8.18 (d, *J* = 7.6 Hz, 2H, ArH), 8.40 (s, 2H, ArH); ^{13}C-NMR (100 MHz, $CDCl_3$): δ 13.3, 19.4, 29.3, 32.1, 44.9, 108.7, 108.9, 118.9, 119.2, 120.4, 122.9, 123.4, 125.1, 125.8, 126.1, 127.6, 129.3, 131.1, 140.9, 141.5, 143.7, 155.6; HRMS *m/z* calcd for ($C_{44}H_{37}N_5$ + H^+): 636.3127; found: 636.3123.

4-Butyl-3,5-bis[4-(9-ethyl-9*H*-carbazol-3-yl)phenyl]-4*H*-1,2,4-triazole (**9i**). Creamy solid in 98% yield, 0.326 g, m.p. 269–270 °C; UV (CH_2Cl_2) λ_{max} 243.0 nm ($\varepsilon \cdot 10^{-3}$ 51.1 $cm^{-1}M^{-1}$), 301.0 (70.7) and 323.0 (47.1); IR (ATR) ν: 3049, 2973, 1740, 1598, 1460, 1379, 1346, 1325, 1295, 1252, 1233, 1197, 1154, 1125, 1087, 848, 804, 769, 747, 730, 694 cm^{-1}; ^{1}H-NMR (400 MHz, $CDCl_3$): δ 0.72 (t, *J* = 7.6 Hz, 3H, CH_3), 1.11 (sext, *J* = 7.6 Hz, 2H, CH_2), 1.46–1.53 (m, 8H, CH_2 + CH_3), 4.24 (t, *J* = 7.6 Hz, 2H, CH_2), 4.42 (q, *J* = 7.2 Hz, 4H, CH_2), 7.28 (t, *J* = 7.6 Hz, 2H, ArH), 7.45 (d, *J* = 7.6 Hz, 2H, ArH), 7.49–7.53 (m, 4H, ArH), 7.78–7.82 (m, 6H, ArH), 7.90 (d, *J* = 8.4 Hz, 4H, ArH), 8.18 (d, *J* = 7.6 Hz, 2H, ArH), 8.40 (s, 2H, ArH); ^{13}C-NMR (100 MHz, $CDCl_3$): δ 13.3, 13.8, 19.4, 32.1, 37.7, 44.9, 108.7, 108.8, 119.0, 119.1, 120.5, 123.0, 123.6, 125.1, 125.8, 126.0, 127.6, 129.3, 131.0, 139.8, 140.4, 143.7, 155.6; HRMS *m/z* calcd for ($C_{46}H_{41}N_5$ + H^+): 664.3440; found: 664.3439.

4-Butyl-3,5-bis[4′-(9*H*-carbazol-9-yl)biphenyl-4-yl]-4*H*-1,2,4-triazole (**9j**). Grey solid in 91% yield, 0.344 g, m.p. 320–323 °C; UV (CH_2Cl_2) λ_{max} 293.0 nm ($\varepsilon \cdot 10^{-3}$ 50.5 $cm^{-1}M^{-1}$) and 320.0 (42.6); IR (ATR) ν: 3054, 2954, 1599, 1521, 1490, 1478, 1451, 1413, 1367, 1334, 1317, 1303, 1226, 1185, 1171, 1004, 974, 826, 771, 743, 719 cm^{-1}; ^{1}H-NMR (400 MHz, $CDCl_3$): δ 0.74 (t, *J* = 7.6 Hz, 3H, CH_3), 1.13 (sext, *J* = 7.6 Hz, 2H, CH_2), 1.52 (quin, *J* = 7.6 Hz, 2H, CH_2), 4.26 (t, *J* = 7.6 Hz, 2H, CH_2), 7.32 (t, *J* = 7.6 Hz, 4H, ArH), 7.45 (t, *J* = 7.6 Hz, 4H, ArH), 7.50 (d, *J* = 7.6 Hz, 4H, ArH), 7.71 (d, *J* = 8.4 Hz, 4H, ArH), 7.85–7.89 (m, 8H, ArH), 7.92 (d, *J* = 8.4 Hz, 4H, ArH), 8.18 (d, *J* = 7.6 Hz, 4H, ArH); ^{13}C-NMR (100 MHz, $CDCl_3$): δ 13.3, 19.4, 32.1, 44.9, 109.8, 120.1, 120.4, 123.5, 126.0, 127.0, 127.5, 127.6, 128.6, 129.5, 137.6, 139.0, 140.8, 141.9, 155.4; HRMS *m/z* calcd for ($C_{54}H_{41}N_5$ + H^+): 760.3440; found: 760.3438.

4-Butyl-3,5-bis[4-(thiantren-1-yl)phenyl]-4*H*-1,2,4-triazole (**9k**). Creamy solid in 86% yield, 0.305 g, m.p. 264–266 °C; UV (CH_2Cl_2) λ_{max} 263.0 nm ($\varepsilon \cdot 10^{-3}$ 66.7 $cm^{-1}M^{-1}$); IR (ATR) ν: 3048, 2952, 2870, 1474, 1441, 1397, 1247, 1188, 1109, 1018, 973, 843, 807, 788, 748, 728, 686 cm^{-1}; ^{1}H-NMR (400 MHz, $CDCl_3$): δ 0.78 (t, *J* = 7.6 Hz, 3H, CH_3), 1.20 (sext, *J* = 7.6 Hz, 2H, CH_2), 1.57 (quin, *J* = 7.6 Hz, 2H, CH_2), 4.29 (t, *J* = 7.6 Hz, 2H, CH_2), 7.21 (t, *J* = 7.6 Hz, 2H, ArH), 7.26 (t, *J* = 7.6 Hz, 2H, ArH), 7.31–7.34 (m, 4H, ArH), 7.37 (d, *J* = 7.6 Hz, 2H, ArH), 7.52 (d, *J* = 7.6 Hz, 2H, ArH), 7.57 (d, *J* = 7.6 Hz, 2H, ArH), 7.60 (d, *J* = 8.4 Hz, 4H, ArH), 7.83 (d, *J* = 8.4 Hz, 4H, ArH); ^{13}C-NMR (100 MHz, $CDCl_3$): δ 13.3, 19.3, 32.1, 44.8, 127.2, 127.7, 127.9, 128.3, 128.6, 128.7, 128.8, 128.9, 129.1, 130.1, 135.1, 135.7, 135.9, 136.2, 141.5, 141.9, 155.4; HRMS *m/z* calcd for ($C_{42}H_{31}N_3S_4$ + H^+): 706.1479; found: 706.1474.

4-Hexyl-3,5-bis[4′-(*N*,*N*-diphenylamino)biphenyl-4-yl]-4*H*-1,2,4-triazole (**10a**). Yellow solid in 61% yield, 0.240 g, m.p. 244–246 °C; UV (CH_2Cl_2) λ_{max} 352.0 nm ($\varepsilon \cdot 10^{-3}$ 68.0 $cm^{-1}M^{-1}$); IR (ATR) ν: 3033, 2925, 2855, 1586, 1508, 1484, 1411, 1328, 1278, 1203, 1173, 1121, 1076, 1025, 1005, 968, 822, 748, 729, 691 cm^{-1}; ^{1}H-NMR (400 MHz, $CDCl_3$): δ 0.73 (t, *J* = 7.2 Hz, 3H, CH_3), 0.99–1.02 (m, 4H, 2 × CH_2), 1.08 (quin, *J* = 7.2 Hz, 2H, CH_2), 1.44 (quin, *J* = 7.2 Hz, 2H, CH_2), 4.16 (t, *J* = 7.2 Hz, 2H, CH_2), 7.06 (t, *J* = 7.2 Hz, 4H, ArH), 7.13–7.18 (m, 12H, ArH), 7.29 (t, *J* = 7.2 Hz, 8H, ArH), 7.55 (d, *J* = 8.4 Hz, 4H, ArH), 7.71–7.75 (m, 8H, ArH); ^{13}C-NMR (100 MHz, $CDCl_3$): δ 13.8, 22.2, 25.7, 29.9, 30.7, 45.0, 123.2, 123.6, 124.6, 126.1, 126.9, 127.8, 129.3, 129.4, 133.5, 142.1, 147.5, 147.9, 155.5; HRMS *m/z* calcd for ($C_{56}H_{49}N_5$ + H^+): 792.4066; found: 792.4061.

3. Results and Discussion

Four basic 4-alkyl-3,5-bis(4-bromophenyl)-4*H*-1,2,4-triazole (**5a–d**) substrates were synthesized starting from 4-bromobenzoic acid (**1**), using our previously elaborated methodologies [58] (Scheme 1). For each reaction, triazole precursors (**5a–d**) containing substituents, differing in their alkyl chain length at the nitrogen atom (position 4), were coupled with 4-(*N*,*N*-diphenylamino)phenylboronic acid (**6a**) in a Suzuki reaction. Transformations were completed using a two-phase solvent system with conventional heating in an oil bath over a sufficiently long period (7 h, TLC) using $Pd(PPh_3)_4$ as a catalyst, and potassium carbonate as a base which gives the desired products in high yields (Scheme 2).

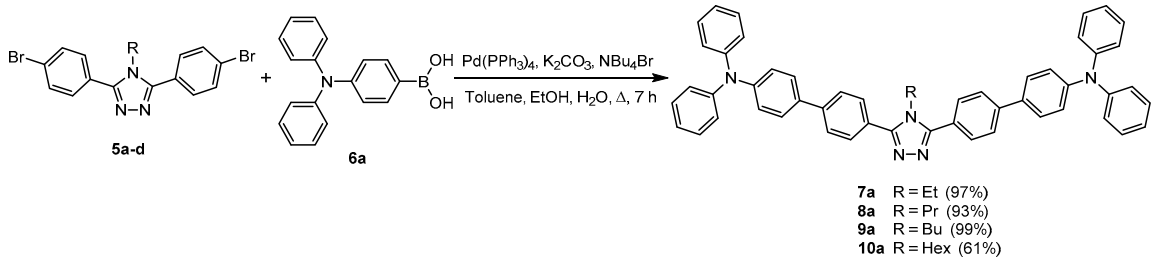

Scheme 2. The conventional Suzuki cross-coupling reaction for 4-alkyl-3,5-bis(4-bromophenyl)-4*H*-1,2,4-triazole derivatives. Reagents and conditions: aryl dibromide **5a–d** (1.00 mmol), 4-(*N*,*N*-diphenylamino)phenylboronic acid (**6a**) (2.50 mmol), $Pd(PPh_3)_4$ (0.05 mmol), NBu_4Br (0.10 mmol), K_2CO_3 (10 mmol), toluene/H_2O/EtOH (10:6:3 mL), oil bath 130 °C, 7 h.

Three (**8a**–**10a**) of the final products form single crystals in the solid-state (Figure 1), enabling the determination of their molecular structures (Table S1). Compounds **8a** and **9a** crystallize as ethanol solvates (Figure S1), while **10a** forms a solventless compound. This is caused by the presence of an *n*-hexyl substituent on the triazole ring of **10a**. The *n*-hexyl terminal methyl and methylene atoms (-CH_2–CH_3) are located in the space occupied by ethanol molecules in **8a** and **9a** (Figures S2–S4). The shorter *n*-butyl and *n*-propyl substituents cannot fill the crystal net space and leave empty voids with volumes of 153–216 Å^3, which are accessible for solvent molecules. Due to discrepancy between the volume of the solvent molecules (~97 Å^3 for one ethanol molecule) and voids, these molecules are disordered in the crystal net (Figures S1 and S5). This affects the neighboring parts of alkyl substituents, which are also disordered in **9a** and **10a** due to the relative freedom of their packing (Figure S1). Compounds **8a** and **9a** in the solid-state are effectively isostructural, whilst **10a** adopts a different packing pattern. In all compounds (**8a–10a**), the molecules extend in one direction of the crystal net, but their mutual shifts are different. In **8a** and **9a,** the subsequent molecules are shifted to approximately half of the preceding molecule length, i.e., the terminal *N*,*N*-diphenylamino group of one molecule is located near the central triazole ring of the neighboring molecule (Figures S2 and S3). In **10a,** the terminal *N*,*N*-diphenylamino groups of the neighboring molecules are adjacent (Figure S4). The overall conformation of molecules **8a–10a** is similar, such that the molecules extend along axes going through the N(triazole)–C(phenylene) bonds due to the presence of 1,4-phenylene moieties. The mutual arrangement of the ring groups is different in all compounds (**8a–10a**), including clearly visible differences in the isostructural **8a** and **9a**. The dihedral angles between the least-squares plane of the diphenylene moiety rings vary from 12.3(1)° to 31.95(6)°, while the angles between the *N*,*N*-diphenylamino moiety rings differ from 52.80(5)° to 66.52(6)° (Table S3). The C–N and N–N bonds with the triazole ring possess similar lengths (Table S2) and respective values are between the length of single and double bonds C–N and N–N, [59] what proves the electron delocalization within the ring. The C(triazole)-C(phenylene) bonds exhibit shortening observed typically in exocyclic bonds connected to aromatic rings [59], which results in the redirecting of the electron density toward the C–C bond. The complete hydrogen bonding scheme of compounds **8a** and **9a** could not be resolved due to the disorder in the solvent molecules' positions. Nevertheless, the studied molecules possess only two classical hydrogen bonds acceptors and non-classical hydrogen bonds donors [60]. The N1 and N2

atoms participate in weak C–H···N hydrogen bonds (Table S4). The isostructural forms of **8a** and **9a** have the same π···π stacking interaction motifs due to the similarity of their crystal packing [61]. One of the phenyl rings from each terminal *N*,*N*-diphenylamino substituent interacts with their symmetry generated equivalent rings. Additionally, one of these rings interacts with the symmetry generated ring of the *N*,*N*-diphenylamino moiety located on the opposite end of the molecule (Table S5). Consequently, one of the four rings belonging to *N*,*N*-diphenylamino substituents interacts with two rings, meaning two interact with one ring, and one does not form any π···π stacking interactions. In **10a,** only two different π···π stacking interactions exist. The first one is formed between the neighboring triazole rings and the second one between one at the phenyl rings of each terminal *N*,*N*-diphenylamino moiety, i.e., similarly to **8a** and **9a**, the phenyl ring of one terminal moiety interacts with the symmetry generated ring of the oppositely located terminal moiety (Table S5).

The final products were tested for their luminescent properties, displaying strong fluorescent properties (Table 1, Figure 2). The compounds have a relatively large Stokes shift ($\Delta\lambda$ = ~90 nm) and a near-unity quantum yield ($\Phi > 0.98$). From these results, an alternative approach to the Suzuki reaction was investigated (Table 2).

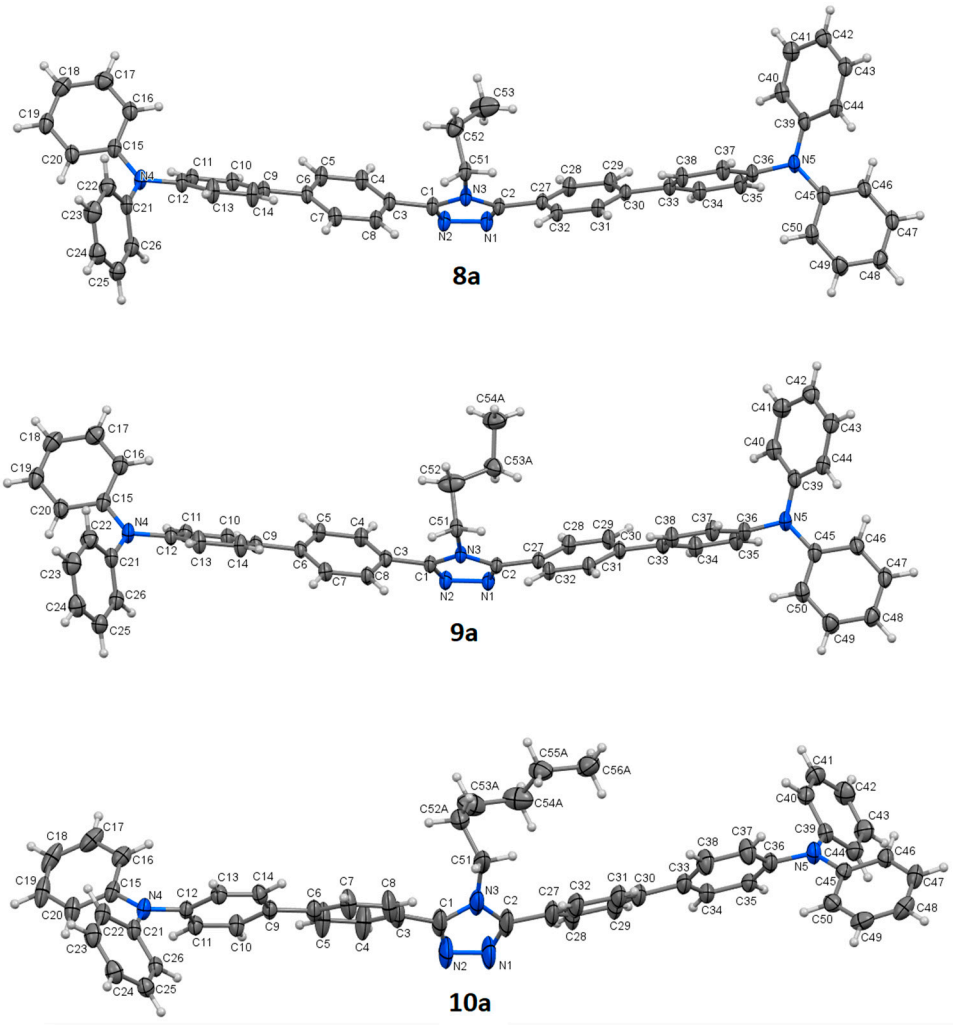

Figure 1. The molecular structures of compounds **8a**–**10a**, with an atom numbering scheme, plotted with a 50% probability of the displacement ellipsoids of non-hydrogen atoms. Hydrogen atoms are plotted as spheres with arbitrary radii. The disordered solvent molecules of **8a** and **9a**, as well as a minor contribution from the distorted alkyl chains of **9a** and **10a**, are omitted for clarity.

Table 1. 4-Alkyl-3,5-bis[4′-(*N*,*N*-diphenylamino)biphenyl-4-yl]-4*H*-1,2,4-triazoles (**7–10a**) prepared using the Suzuki cross-coupling reaction [a].

Product	Yield [a] (%)	Absorption Maximum λ_{max}^{abs} (nm)	Excitation Wavelength λ_{max}^{ex}(nm)	Emission Wavelength λ_{max}^{em}(nm)	Stokes Shift [b] Δ (nm)	Quantum Yield [c,d,e] Φ
7a	97	351	352	443	92	>0.98 [c,d,e]
8a	93	352	352	442	90	>0.98 [c,d,e]
9a	99	351	351	443	92	>0.98 [c,d,e]
10a	61	352	352	443	91	>0.98 [c,d,e]

[a] isolated yield. [b] stokes shift (Δ) from the equation $\Delta = \lambda_{max}^{em} - \lambda_{max}^{abs}$. Wavelength determined from the 3D emission spectrum for C = 5.0×10^{-6} M CH_2Cl_2 solution (nm). [c] quinine sulfate was used as a standard [62]. [d] trans,trans-1,4-diphenyl-1,3-butadiene was used as a standard [63]. [e] exact value cannot be determined due to nonlinearity of standard/sample dependence in the Φ region of 0.97–1.00 [64].

Table 2. An alternative ionic liquids (IL) Suzuki cross-coupling reaction of the 4-alkyl-3,5-bis(4-bromophenyl)-4*H*-1,2,4-triazole moiety (**7a–10a**).

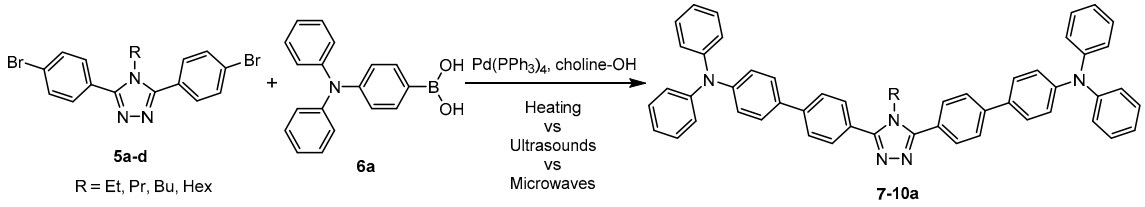

Entry	Substrate	Approach	Reaction Time	Additional Solvent (1 mL)	Yield [a] (%)
1	**5a**	Conventional heating (oil bath 130 °C)	24 h	-	-
2				Toluene	85
3		Ultrasounds	10 h	-	5
4				Toluene	89
5		Microwaves	6 min	-	8
6				Toluene	94
7	**5b**	Conventional heating (oil bath 130 °C)	24 h	-	-
8				Toluene	80
9		Ultrasounds	10 h	-	3
10				Toluene	87
11		Microwaves	6 min	-	10
12				Toluene	89
13	**5c**	Conventional heating (oil bath 130 °C)	24 h	-	-
14				Toluene	85
15		Ultrasounds	10 h	-	3
16				Toluene	93
17		Microwaves	6 min	-	9
18				Toluene	97
19	**5d**	Conventional heating (oil bath 130 °C)	24 vh	-	-
20				Toluene	47
21		Ultrasounds	10 h	-	-
22				Toluene	56
23		Microwaves	6 min	-	5
24				Toluene	62

[a] yield with respect to the 4-alkyl-3,5-bis(4-bromophenyl)-4*H*-1,2,4-triazole (**5a–d**). Reagents and conditions: aryl dibromide **5a–d** (1.00 mmol), boronic acid **6a** (2.50 mmol), $Pd(PPh_3)_4$ (0.05 mmol), choline–OH (10 mL).

The use of ionic liquids in the Suzuki cross-coupling reaction opens up the possibility for the additional acceleration of the reaction with the use of ultrasound or microwaves. These variants

(Table 2, entries: 3–6, 9–12, 15–18 and 21–24) have a shorter reaction time compared to conventional heating (Table 2, entries: 1, 2, 7, 8, 13, 14, 19 and 20) in an oil bath while maintaining a high coupling efficiency. The most beneficial aspects from an economic point of view is the use of a small addition of a classical solvent (toluene, 1 mL) and conducting the reaction in a microwave reactor, where the complete conversion of substrates takes place after only 6 min (TLC), and the products are obtained in high yields (Table 2, entries: 6, 12, 18 and 24, 62–97%).

The highest yields were obtained for derivatives with two and four carbon alkyl chains, the subsequent reactions were carried out for these two series of triazole precursors, **5a** and **5c** (Scheme 3), and then their emission properties were tested (Table 3). Generally, compounds containing a 4*H*-1,2,4-triazole core substituted with an ethyl group at the position 4 were synthesized with a slightly smaller range of yields (70–99% for **7a–k**, Tables 1 and 3) than their counterparts with the butyl substituent (62–99% for **9a–k**, Tables 1 and 3).

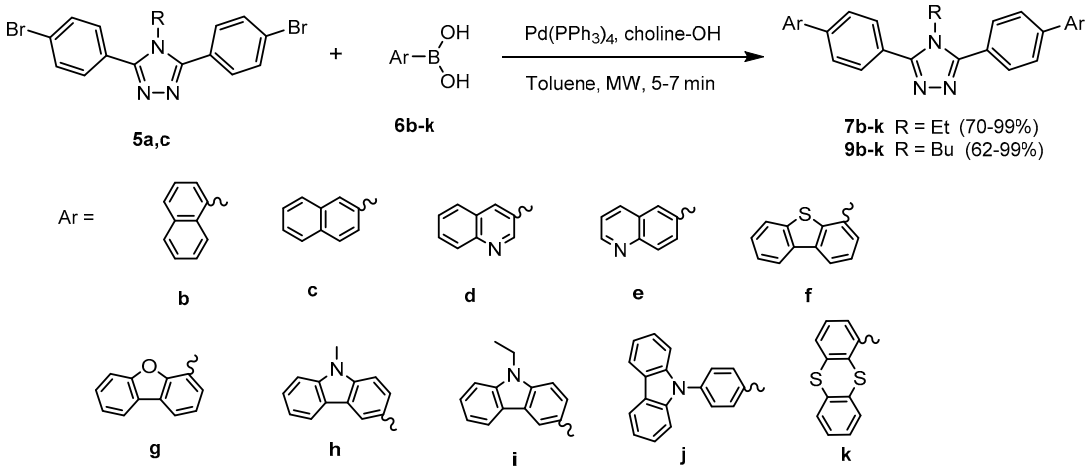

Scheme 3. The Suzuki coupling reaction of 4*H*-1,2,4-triazole precursors **5a** and **5c** with selected boronic acids **6b–k**. Reagents and conditions: aryl dibromide **5a,c** (1.00 mmol), arylboronic acid **6b–k** (2.50 mmol), $Pd(PPh_3)_4$ (0.05 mmol), choline–OH/toluene (10:1 mL), and microwave irradiation, 5–7 min.

Three-dimensional fluorescence characteristics were determined for all the final products from the outlined reactions. The spectra of compounds **7a–7e**, **8a**, **9a–9e** and **10a** possess a single fluorescence maximum, while compounds **7f–7k** and **9f–9k** have two maxima (Figures 2–4). Almost all of the synthesized compounds emit strong fluorescence upon irradiation with UV light. The only exceptions are the compounds **7k** and **9k** containing the thianthrene substituent (Table 3). This is due to the presence of two sulfur atoms in the thianthrene moiety. Typically, the presence of one sulfur atom in a molecule causes the severe quenching of fluorescence [65,66]. In each molecule of compound **7k** and **9k,** four sulfur atoms are present, thus, the almost total quenching of fluorescence is observed (Figures 3 and 4). Similarly, the existence of two sulfur atoms per one molecule in **7f** and **9f** distinctly decreases the number of emitted photons in comparison to the other studied compounds without a sulfur atom in the structure. The change in the aliphatic substituent length at the triazole nitrogen N atom does not affect the position and shape of the three-dimensional emission maxima. The effect of increased emission wavelengths for aliphatic substituents with even number of carbon atoms (in comparison to these with odd number of carbon atoms) is not observed in the studied case [58]. This suggests that the presence of substituents containing a single ring at the ends of the 4-alkyl-3,5-bis(phenyl)-4*H*-1,2,4-triazole core is necessary for the aforementioned even/odd number of carbon atoms and its influence on fluorescence. In the studied compounds, the terminal substituents consists of two up to four rings (in the subsequent or fused arrangement) and this completely diminishes the effect of the aliphatic substituent parity at the triazole nitrogen N atom.

Table 3. 4-Alkyl-3,5-bis(4-arylphenyl)-4*H*-1,2,4-triazoles **7b–k** and **9b–k** prepared using the Suzuki cross-coupling reaction [a].

Product	Yield [a] (%)	Absorption Maximum λ_{max}^{abs} (nm)	Excitation Wavelength λ_{max}^{ex}(nm)	Emission Wavelength λ_{max}^{em}(nm)	Stokes Shift [b] Δ (nm)	Quantum Yield [c,d,e] Φ
7b	88	297	304	382	85	0.75 [c]/0.74 [d]
7c	99	305	313	394	89	>0.98 [c,d,e]
7d	79	305	312	395	90	0.75 [c]/0.74 [d]
7e	94	306	312	394	88	0.55 [c]/0.54 [d]
7f	96	290 335	291 335	371 374	81 39	0.11 [c]/0.11 [d] 0.18 [c]/0.18 [d]
7g	92	286 315	290 316	388 388	102 73	0.63 [c]/0.62 [d] 0.95 [c]/0.93 [d]
7h	70	300 321	304 322	403 401	103 80	0.77 [c]/0.76 [d] >0.98 [c,d,e]
7i	76	301 322	304 322	404 403	103 81	0.78 [c]/0.77 [d] >0.98 [c,d,e]
7j	77	293 322	293 328	409 408	116 86	0.77 [c]/0.76 [d] >0.98 [c,d,e]
7k	87	263	-	-	-	-
9b	62	296	304	382	86	0.64 [c]/0.62 [d]
9c	89	305	313	393	88	0.95 [c]/0.93 [d]
9d	99	304	311	395	91	0.40 [c]/0.39 [d]
9e	91	306	313	393	87	0.60 [c]/0.58 [d]
9f	93	290 335	291 335	373 376	83 41	0.14 [c]/0.14 [d] 0.27 [c]/0.26 [d]
9g	88	286 317	292 318	387 388	101 71	0.76 [c]/0.75 [d] >0.98 [c,d,e]
9h	97	300 323	304 323	402 402	102 79	0.80 [c]/0.78 [d] >0.98 [c,d,e]
9i	98	301 323	304 323	403 402	102 79	0.78 [c]/0.77 [d] >0.98 [c,d,e]
9j	91	293 320	295 327	409 408	116 88	0.81 [c]/0.79 [d] >0.98 [c,d,e]
9k	86	263	-	-	-	-

[a] isolated yield. [b] stokes shift (Δ) from the equation $\Delta = \lambda_{max}^{em} - \lambda_{max}^{abs}$. Wavelength determined from the 3D emission spectrum for C = 5.0×10^{-6} M CH_2Cl_2 solution (nm). [c] quinine sulfate was used as a standard [62]. [d] trans,trans-1,4-diphenyl-1,3-butadiene was used as a standard [63]. [e] exact value cannot be determined due to the nonlinearity of standard/sample dependence in the Φ region 0.97–1.00 [64].

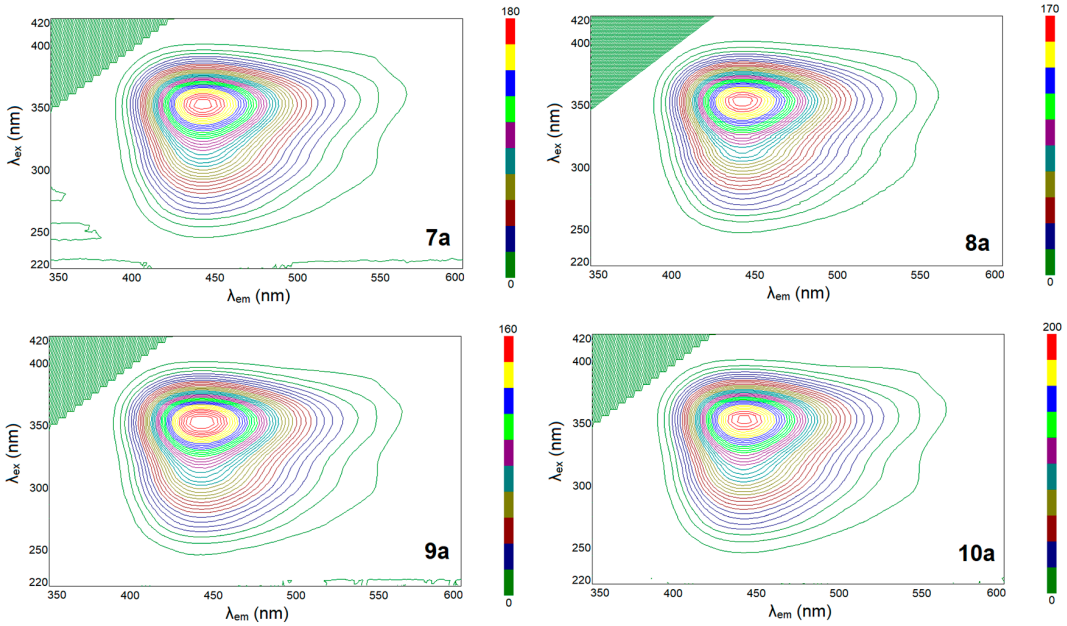

Figure 2. Three-dimensional fluorescence spectra of compounds **7a**–**10a**. The color scale represents the flux of emitted photons. The number above the color scales indicates the maximum relative value of emission intensity represented by color scale (and indicated in the respective figure). The unit of measurement in each spectrum represents the same number of emitted photons per second, i.e., all values of intensity presented in Figures 2–4 can be directly compared. The green area (upper left triangles in each spectrum) indicates the non-fluorescent region in which λ_{ex} is close to or larger than λ_{em}.

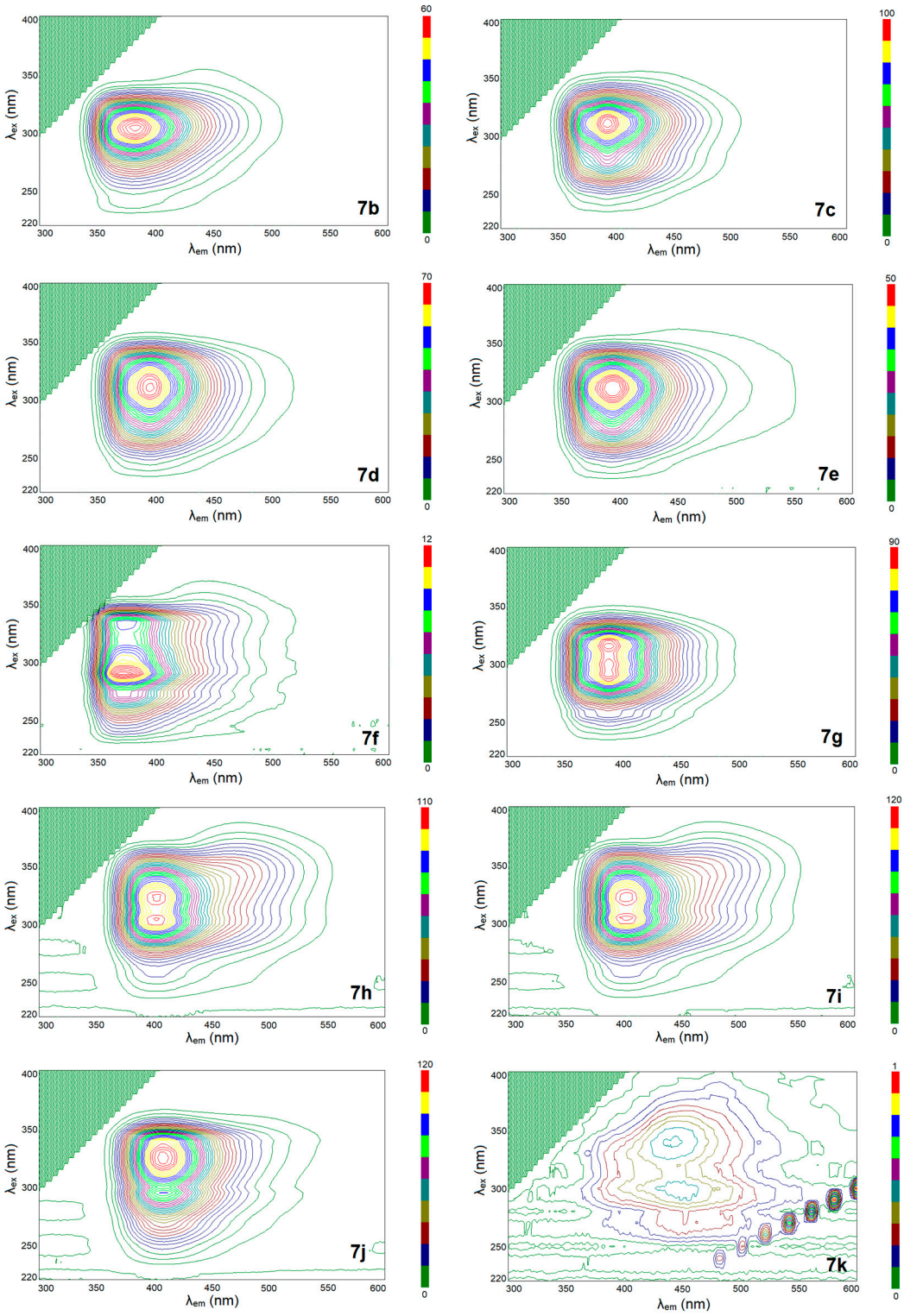

Figure 3. Three-dimensional fluorescence spectra of compounds **7b**–**7k**. The color scale represents the flux of emitted photons. The number above the color scales indicates the maximum relative value of emission intensity represented by color scale (and indicated in the respective figure). The unit of measurement in each spectrum represents the same number of emitted photons per second, i.e., all values of intensity presented in Figures 2–4 can be directly compared. The green area (upper left triangles in each spectrum) indicates the non-fluorescent region in which λ_{ex} is close to or larger than λ_{em}.

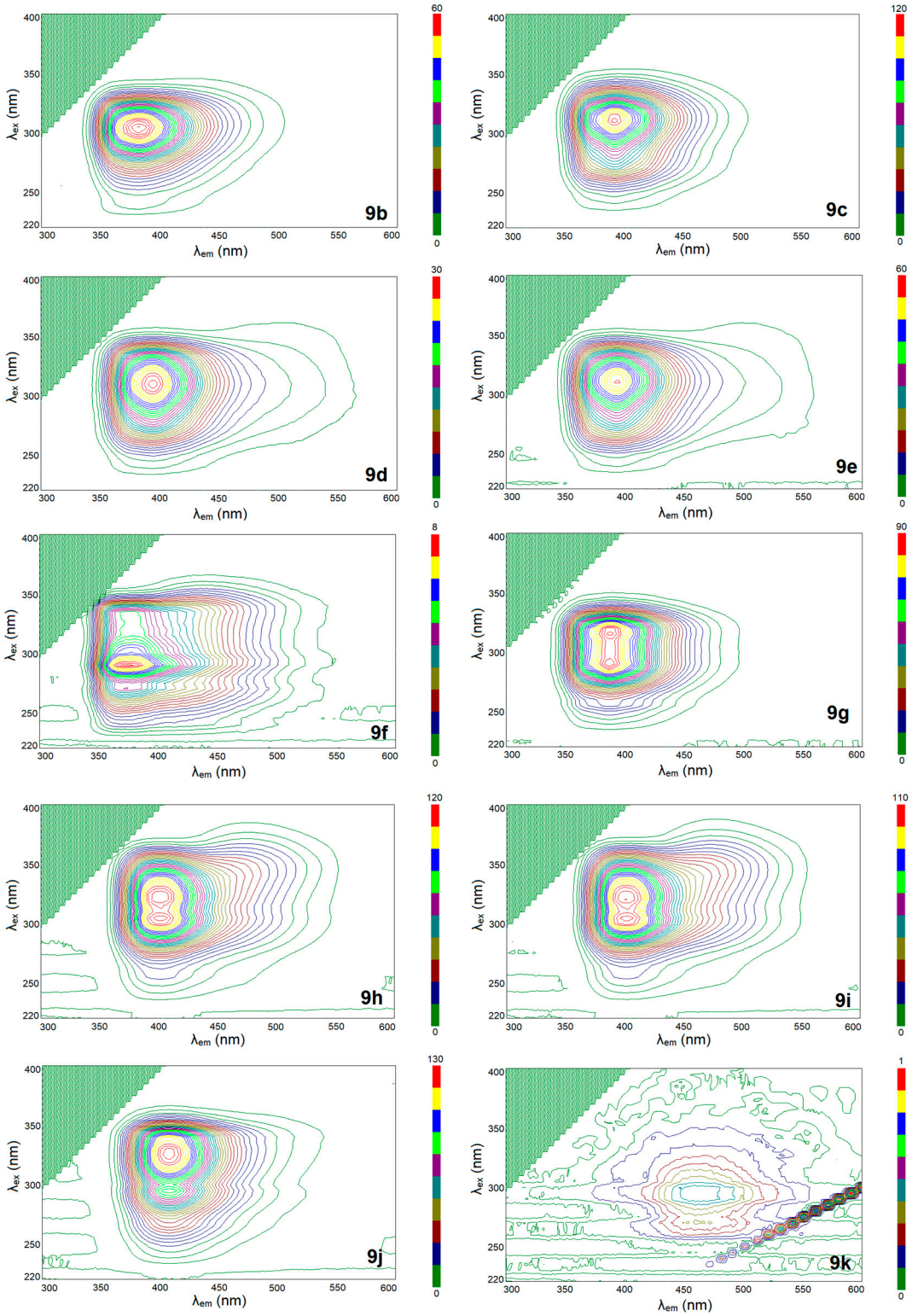

Figure 4. Three-dimensional fluorescence spectra of compounds **9b**–**9k**. The color scale represents the flux of emitted photons. The number above the color scales indicates the maximum relative value of emission intensity represented by color scale (and indicated in the respective figure). The unit of measurement in each spectrum represents the same number of emitted photons per second, i.e., all values of intensity presented in Figures 2–4 can be directly compared. The green area (upper left triangles in each spectrum) indicates the non-fluorescent region in which λ_{ex} is close to or larger than λ_{em}.

The number of rings in terminal substituents also affects the excitation and emission wavelengths (Figure S8). There is a decrease in the excitation wavelength for the first maximum on the spectrum (accompanied by an increase in the excitation wavelength for the second maximum on the spectrum) with an increase in the number of rings (Figure S8). The difference between the excitation and emission wavelengths at the maxima falls by approximately 70–84 nm (for compounds possessing two fluorescence maxima, at least one fulfills this relation), thus the energy gap between the respective orbitals responsible for the fluorescence is very similar in all studied compounds. The spectra of the compounds with rings separated by a single bond (**7a–10a**) or with no more than two fused rings (**7b–7e** and **9b–9e**) possess a single maximum in the three-dimensional fluorescence spectrum. The compounds with three fused rings (**7f–7k** and **9f–9k**) possess two more or less shaped maxima at the same emission wavelength and two different excitation wavelengths. Manifestations of these maxima were faintly but unambiguously visible in the compounds with almost completely quenched fluorescence (**7k** and **9k**). All the single maxima possess a considerable degree of asymmetry, with the emission drastically fading with a decrease in the emission wavelengths and/or increase in the excitation wavelengths. In two other directions of the spectra, the emission decreases slowly. This originates from the electronic transitions of the excited state (S_1) to the different energy sub-levels (vibrational energy levels 0, 1, 2, . . .) of the ground state (S_0). The asymmetricity increases with the number of electrons in the delocalized system (**7b** ≈ **7c** ≈ **9b** ≈ **9c** < **7d** ≈ **7e** ≈ **9d** ≈ **9e** < **7a** ≈ **8a** ≈ **9a** ≈ **10a**), due to the increased number of vibrational energy levels. The presence of two fluorescence maxima in the spectra of compounds **7f–7k** and **9f–9k** is caused by the presence of ring systems possessing two different heteroatomic rings (central and terminal ones). The intensity of both maxima is similar for compounds **7g–7j** and **9g–9j**. For compounds **7f** and **9f,** the first (at lower excitation wavelengths) maxima is stronger than the second one (existing at larger excitation wavelengths), while for compounds **7j** and **9j** the mutual relation of maxima intensities is reversed. This effect is caused by the presence of a thiophene moiety in the thianthrene ring system of **7f** and **9f** and an occurrence of an additional phenylene moiety in **7j** and **9j** (in comparison to the other studied compounds). The conjugation of the triazole ring with appropriately selected substituents containing together more than six aromatic rings (**7a–10a**, **7g–7j**, and **9g–9j** excluding **7f**, **7k**, **9f**, and **9k,** containing sulfur atoms) leads to reach a nearly 1.00 value of quantum yield (Φ). Such properties are not achieved by triazoles conjugated with four aromatic rings [58]. Their Φ, although high, reaches values maximally around 0.9. The triazoles which are not bonded directly to aryl substituents are characterized by a very low Φ (below 0.01) [67]. To improve the fluorescence properties of triazoles conjugated with a lower number of aromatic rings, the coordination compounds with d^{10} transition metals are synthesized [68]. Even then, the zinc compounds of triazoles with one aromatic ring achieve Φ only up to 0.075 [69]. The Φ of the studied compounds correlate well with the fluorescence intensities (larger fluorescence leads to larger Φ, Figure S9), whereas there is no discernible relationship between Φ and absorption (Figure S10). This suggests that the mechanism of fluorescence is similar in all compounds and the relatively large differences in the absorption values derive from the variations in the amount of electromagnetic energy (photons) transformed directly into internal energy. The above described effects (presence/lack of a correlation) exist also in 4-alkyl-3,5-bis(phenyl)-4*H*-1,2,4-triazole substituted at the ends by a single ring [58] and there is no such effects in the di(1,3,4-oxadiazol-2-yl)-1,2,4,5-tetrazine and 3,6-di(1,3,4-thiadiazol-2-yl)-1,2,4,5-tetrazine derivatives [70]. In the case of the compounds exhibiting a single fluorescence maximum, the n→π^* absorption transition is the main source of the excited states leading to the subsequent emission of the fluorescence photons. The origin of fluorescence in the compounds exhibiting two fluorescence maxima are n→π^* (for higher λ_{max}^{ex}) and π→π^* (for lower λ_{max}^{ex}) absorption transitions [68]. The involved n-type orbital originates from the nitrogen atom of the triazole ring (N1 or N2) and the source of the π-type orbital is also the triazole ring [71]. The lowest unoccupied molecular orbital in similarly conjugated 1,2,4-triazole compounds is antibonding delocalized orbital (π^*), which most often is the benzene ring directly attached to the triazole ring [72] or fused π^* orbital of triazole and the neighboring benzene [73]. The presence of a single fluorescence maximum or two fluorescence maxima of the same

emission wavelength indicates that $\pi^* \rightarrow \pi$ transitions are responsible for the fluorescence in the studied compounds [74]. Noteworthy is the fact that upon ultraviolet irradiation, the compounds **7a–10a** emit a strong deep-blue fluorescence light visible by the naked eye. The blue-violet color emitted light is clearly visible for compound **7c–7e, 7h–7j, 9c–9e, 9h–9j**.

4. Conclusions

Four alternative approaches using palladium-catalyzed Suzuki cross-coupling reactions to synthesize a series of highly-conjugated 4*H*-1,2,4-triazole derivatives were presented. The reactions of the intermediate 4-alkyl-3,5-bis(4-bromophenyl)-4*H*-1,2,4-triazoles and boronic acids were conducted using conventional heating in a two-phase solvent system (toluene/EtOH/H_2O) or using an ionic liquid (choline–OH). For the ionic liquid approach, it was possible to use ultrasound or microwave assistance, which significantly reduces the reaction time. Additionally, this type of methodology removes the need for large amounts of organic solvents and for the addition of auxiliary reagents such as a base or a phase transfer catalyst. Generally, 4-alkyl-4*H*-1,2,4-triazole derivatives conjugated to different fused-bicyclic and fused-tricyclic systems via a 1,4-phenylene linker were obtained in excellent yields. Almost all compounds are effective fluorophores and emit visible light upon irradiation by ultraviolet electromagnetic waves. The exceptions are the products possessing sulfur atoms within terminal moieties, which cause a large decrease in the fluorescence. The studied compounds produce fluorescence with large quantum yields (up to almost 100%), which depend on a structure of the terminal substituents. The obtained compounds, due to their good emission properties and relatively good solubility in typical organic solvents, seem to be of particular interest for optoelectronic purposes.

Supplementary Materials: The following are available online at http://www.mdpi.com/1996-1944/13/24/5627/s1, copy of ^{1}H NMR, ^{13}C NMR and HRMS spectra; X-ray crystallography data; absorption spectrometry data. Figure S1: Complete asymmetric units of the structures of compounds **8a**, **9a**, and **10a**, with atom numbering scheme, plotted with 50% probability of displacement ellipsoids of non-hydrogen atoms. Hydrogen atoms are plotted as spheres of arbitrary radii, Figure S2: Solvent accessible voids within crystal structure of **8a**, Figure S3: Solvent accessible voids within crystal structure of **9a**, Figure S4: The part of crystal packing in **10a**, Figure S5: Disorder model of solvent in **8a**, Figure S6: UV-Vis spectra of **7a–10a** and **7b–7k**, Figure S7: UV-Vis spectra of **9b–9k**, Figure S8: Positions of global maxima for studied compounds (divided into groups containing 2 or 3 rings at the ends of 4-alkyl-3,5-bis(phenyl)-4*H*-1,2,4-triazole core). "1st max." and "2nd max." indicate the first (for smaller excitation wavelengths) and the second (for larger excitation wavelengths) maxima on three-dimensional fluorescence spectra, Figure S9: Quantum yield of studied compounds as a function of fluorescence intensity at global and local maximum, Figure S10: Quantum yield of studied compounds in relation to absorption at global and local maximum of fluorescence, Table S1: Crystal data and structure refinement details for **8a**, **9a**, and **10a**. The structures of **8a** and **9a** were refined twice: against measured and squeezed data, Table S2: Selected structural data of **8a**, **9a**, and **10a**, Table S3: Dihedral angles (°) between ring least squares planes in **8a**, **9a**, and **10a**. Each ring is indicated by one atom, which belongs solely to this ring, Table S4: Non-classic hydrogen bonds and the first level graph motifs in the studied compounds (Å, °), Table S5: Stacking interactions in the studied compounds. Each ring is indicated by one atom, which belongs solely to this ring. The α is a dihedral angle between planes I and J, β is an angle between Cg(I)-Cg(J) vector and normal to plane I, d_p is a perpendicular distance of Cg(I) on ring J plane.

Author Contributions: Conceptualization, M.O. and A.K.; methodology, M.O. and A.K.; formal analysis, M.O. and M.Ś.; investigation, M.O.; data curation, M.Ś.; writing—original draft preparation, M.O. and M.Ś.; writing—review and editing, A.K. All authors have read and agreed to the published version of the manuscript.

Funding: This research was funded by Polish National Science Centre grant UMO-2016/23/N/ST5/02036.

Acknowledgments: The authors would like to thank the late Rafał Kruszyński for his contribution to this project.

Conflicts of Interest: The authors declare no conflict of interest.

References

1. Kraft, A.; Grimsdale, A.C.; Holmes, A.B. Electroluminescent Conjugated Polymers—Seeing Polymers in a New Light. *Angew. Chem. Int. Ed.* **1998**, *37*, 402–428. [CrossRef]
2. Segura, J.L. The chemistry of electroluminescent organic materials. *Acta Polym.* **1998**, *49*, 319–344. [CrossRef]

3. Mitschke, U.; Bäuerle, P. The electroluminescence of organic materials. *J. Mater. Chem.* **2000**, *10*, 1471–1507. [CrossRef]
4. Bera, M.K.; Pal, P.; Malik, S. Solid-state emissive organic chromophores: Design, strategy and building blocks. *J. Mater. Chem. C* **2020**, *8*, 788–802. [CrossRef]
5. Zhu, M.; Yang, C. Blue fluorescent emitters: Design tactics and applications in organic light-emitting diodes. *Chem. Soc. Rev.* **2013**, *42*, 4963–4976. [CrossRef] [PubMed]
6. Katritzky, A.R.; Ramsden, C.A.; Joule, J.A.; Zhdankin, V.V. Structure of Five-membered Rings with Two or More Heteroatoms. In *Handbook of Heterocyclic Chemistry*; Elsevier: Oxford, UK, 2010; Volume 2, pp. 139–209.
7. Curtis, A.D.M.; Jennings, N. 1,2,4-Triazoles. In *Comprehensive Heterocyclic Chemistry III*; Katritzky, A.R., Ramsden, C.A., Scriven, E.F.V., Taylor, R.J.K., Eds.; Elsevier: Oxford, UK, 2008; Volume 5, pp. 159–209.
8. Liu, H.; Wang, L.; Wu, Y.; Liao, Q. Luminescence emission-modulated based on specific two-photon compound of triazole-conjugated pyrene derivative. *RSC Adv.* **2017**, *7*, 19002–19006. [CrossRef]
9. Li, W.; Yan, L.; Zhou, H.; You, W. A General Approach toward Electron Deficient Triazole Units to Construct Conjugated Polymers for Solar Cells. *Chem. Mater.* **2015**, *27*, 6470–6476. [CrossRef]
10. Wu, C.-S.; Lee, S.-L.; Chen, Y. Bipolar copoly(aryl ether) containing distyrylbenzene, triphenylamine, and 1,2,4-triazole moieties: Synthesis and optoelectronic properties. *J. Polym. Sci. Part A Polym. Chem.* **2011**, *49*, 3099–3108. [CrossRef]
11. Tao, Y.; Wang, Q.; Ao, L.; Zhong, C.; Yang, C.; Qin, J.; Ma, D. Highly Efficient Phosphorescent Organic Light-Emitting Diodes Hosted by 1,2,4-Triazole-Cored Triphenylamine Derivatives: Relationship between Structure and Optoelectronic Properties. *J. Phys. Chem. C* **2010**, *114*, 601–609. [CrossRef]
12. Meng, X.; Chen, M.; Bai, R.; He, L. Cationic Iridium Complexes with 3,4,5-Triphenyl-4 H-1,2,4-Triazole Type Cyclometalating Ligands: Synthesis, Characterizations, and Their Use in Light-Emitting Electrochemical Cells. *Inorg. Chem.* **2020**, *59*, 9605–9617. [CrossRef]
13. Demirbaş, Ü.; Özçifçi, Z.; Akçay, H.T.; Menteşe, E. Novel phthalocyanines bearing 1,2,4 triazole substituents: Synthesis, characterization, photophysical and photochemical properties. *Polyhedron* **2020**, *181*, 114470. [CrossRef]
14. Abdurahman, A.; Wang, L.; Zhang, Z.; Feng, Y.; Zhao, Y.; Zhang, M. Novel triazole-based AIE materials: Dual-functional, highly sensitive and selective fluorescence probe. *Dye. Pigment.* **2020**, *174*, 108050. [CrossRef]
15. Yan, Y.; Lin, X.; Zhang, L.; Zhou, H.; Wu, L.; Cai, L. Electrochemical and quantum-chemical study on newly synthesized triazoles as corrosion inhibitors of mild steel in 1 M HCl. *Res. Chem. Intermed.* **2017**, *43*, 3145–3162. [CrossRef]
16. Jiang, L.; Lan, Y.; He, Y.; Li, Y.; Li, Y.; Luo, J. 1,2,4-Triazole as a corrosion inhibitor in copper chemical mechanical polishing. *Thin Solid Films* **2014**, *556*, 395–404. [CrossRef]
17. Sherif, E.-S.M.; Erasmus, R.M.; Comins, J.D. Effects of 3-amino-1,2,4-triazole on the inhibition of copper corrosion in acidic chloride solutions. *J. Colloid Interface Sci.* **2007**, *311*, 144–151. [CrossRef]
18. Wang, L. Inhibition of mild steel corrosion in phosphoric acid solution by triazole derivatives. *Corros. Sci.* **2006**, *48*, 608–616. [CrossRef]
19. Shet, N.; Nazareth, R.; Suchetan, P.A. Corrosion inhibition of 316 stainless steel in 2M HCl by 4-{[4-(dimethylamino)benzylidene]amino}-5-methyl-4H-1,2,4-triazole-3-thiol. *Chem. Data Collect.* **2019**, *20*, 100209. [CrossRef]
20. He, P.; Wu, B.; Shao, S.; Teng, T.; Wang, P.; Qu, X.-P. Characterization of 1,2,4-Triazole as Corrosion Inhibitor for Chemical Mechanical Polishing of Cobalt in H_2O_2 Based Acid Slurry. *ECS J. Solid State Sci. Technol.* **2019**, *8*, P3075–P3084. [CrossRef]
21. Zhang, J.; Wang, S.; Ba, Y.; Xu, Z. 1,2,4-Triazole-quinoline/quinolone hybrids as potential anti-bacterial agents. *Eur. J. Med. Chem.* **2019**, *174*, 1–8. [CrossRef]
22. Gao, F.; Wang, T.; Xiao, J.; Huang, G. Antibacterial activity study of 1,2,4-triazole derivatives. *Eur. J. Med. Chem.* **2019**, *173*, 274–281. [CrossRef]
23. Venugopala, K.N.; Kandeel, M.; Pillay, M.; Deb, P.K.; Abdallah, H.H.; Mahomoodally, M.F.; Chopra, D. Anti-Tubercular Properties of 4-Amino-5-(4-Fluoro-3-Phenoxyphenyl)-4H-1,2,4-Triazole-3-Thiol and Its Schiff Bases: Computational Input and Molecular Dynamics. *Antibiotics* **2020**, *9*, 559. [CrossRef] [PubMed]

24. Mehta, C.C.; Patel, A.; Bhatt, H.G. New molecular insights into dual inhibitors of tankyrase as Wnt signaling antagonists: 3D-QSAR studies on 4H-1,2,4-triazole derivatives for the design of novel anticancer agents. *Struct. Chem.* **2020**, *31*, 2371–2389. [CrossRef]
25. Saadaoui, I.; Krichen, F.; Ben Salah, B.; Ben Mansour, R.; Miled, N.; Bougatef, A.; Kossentini, M. Design, synthesis and biological evaluation of Schiff bases of 4-amino-1,2,4-triazole derivatives as potent angiotensin converting enzyme inhibitors and antioxidant activities. *J. Mol. Struct.* **2019**, *1180*, 344–354. [CrossRef]
26. Fan, Y.-L.; Ke, X.; Liu, M. Coumarin-triazole Hybrids and Their Biological Activities. *J. Heterocycl. Chem.* **2018**, *55*, 791–802. [CrossRef]
27. Kaur, P.; Chawla, A. 1,2,4-Triazole: A Review Of Pharmacological Activities. *Parminder Kaur Anshul Chawla. Int. Res. J. Pharm* **2017**, *8*, 10–29. [CrossRef]
28. Zhang, S.; Xu, Z.; Gao, C.; Ren, Q.-C.; Chang, L.; Lv, Z.-S.; Feng, L.-S. Triazole derivatives and their anti-tubercular activity. *Eur. J. Med. Chem.* **2017**, *138*, 501–513. [CrossRef] [PubMed]
29. Asif, M. Biological Potentials of Biological Active Triazole Derivatives: A Short Review. *Org. Chem. Curr. Res.* **2016**, *5*, 1000173. [CrossRef]
30. Maddila, S.; Pagadala, R.; Jonnalagadda, S. 1,2,4-Triazoles: A Review of Synthetic Approaches and the Biological Activity. *Lett. Org. Chem.* **2013**, *10*, 693–714. [CrossRef]
31. Zhou, C.-H.; Wang, Y. Recent Researches in Triazole Compounds as Medicinal Drugs. *Curr. Med. Chem.* **2012**, *19*, 239–280. [CrossRef]
32. Sever, B.; Altıntop, M.D.; Demir, Y.; Pekdoğan, M.; Akalın Çiftçi, G.; Beydemir, Ş.; Özdemir, A. An extensive research on aldose reductase inhibitory effects of new 4H-1,2,4-triazole derivatives. *J. Mol. Struct.* **2020**, 129446. [CrossRef]
33. Hull, J.W.; Romer, D.R.; Adaway, T.J.; Podhorez, D.E. Development of Manufacturing Processes for a New Family of 2,6-Dihaloaryl 1,2,4-Triazole Insecticides. *Org. Process Res. Dev.* **2009**, *13*, 1125–1129. [CrossRef]
34. Zhang, Z.; Gao, B.; He, Z.; Li, L.; Shi, H.; Wang, M. Enantioselective metabolism of four chiral triazole fungicides in rat liver microsomes. *Chemosphere* **2019**, *224*, 77–84. [CrossRef] [PubMed]
35. Li, J.; Ren, G.-Y.; Zhang, Y.; Yang, M.-Y.; Ma, H.-X. Two Cu(II) complexes of 1,2,4-triazole fungicides with enhanced antifungal activities. *Polyhedron* **2019**, *157*, 163–169. [CrossRef]
36. Verweij, P.E.; Kema, G.H.; Zwaan, B.; Melchers, W.J. Triazole fungicides and the selection of resistance to medical triazoles in the opportunistic mould Aspergillus fumigatus. *Pest Manag. Sci.* **2013**, *69*, 165–170. [CrossRef] [PubMed]
37. Ribas e Ribas, A.D.; Spolti, P.; Del Ponte, E.M.; Donato, K.Z.; Schrekker, H.; Fuentefria, A.M. Is the emergence of fungal resistance to medical triazoles related to their use in the agroecosystems? A mini review. *Braz. J. Microbiol.* **2016**, *47*, 793–799. [CrossRef]
38. Lohmann, J.K.; Craig, I.R.; Brahm, L.; Fehr, M.; Weber, A.; Seet, M.; Mueller, B.; Wiebe, C.; Winter, C.H.; Grote, T.; et al. *European Patent Application Substituted [1,2,4]triazoles as Agricultural Fungicides*; European Patent Organisation: Dallas, TX, USA, 2020; pp. 1–79.
39. Shalini, K.; Kumar, N.; Drabu, S.; Sharma, P.K. Advances in synthetic approach to and antifungal activity of triazoles. *Beilstein J. Org. Chem.* **2011**, *7*, 668–677. [CrossRef]
40. Moulin, A.; Bibian, M.; Blayo, A.-L.; El Habnouni, S.; Martinez, J.; Fehrentz, J.-A. Synthesis of 3,4,5-Trisubstituted-1,2,4-triazoles. *Chem. Rev.* **2010**, *110*, 1809–1827. [CrossRef]
41. Mustafa, S.; Nair, V.; Chittoor, J.; Krishnapillai, S. Synthesis of 1,2,4-Triazoles and Thiazoles from Thiosemicarbazide and its Derivatives. *Mini Rev. Org. Chem.* **2004**, *1*, 375–385. [CrossRef]
42. Ibrahim, M.A.; El-Gohary, N.M. Heterocyclization with Some Heterocyclic Diamines: Synthetic Approaches for Nitrogen Bridgehead Heterocyclic Systems. *Heterocycles* **2014**, *89*, 1125–1157. [CrossRef]
43. Al-Masoudi, I.A.; Al-Soud, Y.A.; Al-Salihi, N.J.; Al-Masoudi, N.A. 1,2,4-Triazoles: Synthetic approaches and pharmacological importance. (Review). *Chem. Heterocycl. Compd.* **2006**, *42*, 1377–1403. [CrossRef]
44. Jilloju, P.C.; Vinaykumar, A.; Shyam, P.; Vedula, R.R. One-pot, Multicomponent Cascade Reaction for the Synthesis of Various Aralkyl/alkylthio-3,5-dimethyl-1H-pyrazolyl-4H-1,2,4-triazol-4-amine and Their Docking Studies. *J. Heterocycl. Chem.* **2019**, *56*, 1012–1019. [CrossRef]
45. Nikpassand, M.; Farshami, M.J. One-Pot Synthesis of Novel 3-Pyrazolyl-4H-1,2,4-triazoles Using Amino Glucose-Functionalized Silica-Coated NiFe2O4 Nanoparticles as a Magnetically Separable Catalyst. *J. Clust. Sci.* **2020**, 1–8. [CrossRef]

46. Jilloju, P.C.; Srikanth, M.; Kumar, S.V.; Vedula, R.R. One-Pot, Multi-Component Synthesis of Substituted 2-(6-Phenyl-7H-[1,2,4]Triazolo[3,4-b][1,3,4]Thiadiazin-3-yl)-2,3-Dihydrophthalazine-1,4-Diones. *Polycycl. Aromat. Compd.* **2020**, 1–12. [CrossRef]
47. de Meijere, A.; Diederich, F. *Metal-Catalyzed Cross-Coupling Reactions*; de Meijere, A., Diederich, F., Eds.; Wiley-VCH: Weinheim, Germany, 2004; Volume 1.
48. Miyaura, N. Metal-Catalyzed Cross-Coupling Reactions of Organoboron Compounds with Organic Halides. In *Metal-Catalyzed Cross-Coupling Reactions*; de Meijere, A., Diederich, F., Eds.; Wiley-VCH: Weinheim, Germany, 2008; pp. 41–123.
49. Peruzzini, M.; Gonsalvi, L. Phosphorus Compounds. Advanced Tools in Catalysis and Material Sciences. In *Catalysis by Metal Complexes*; Springer: Berlin/Heidelberg, Germany, 2011; Volume 37.
50. Mandal, B.; Ghosh, S.; Basu, B. Task-Specific Properties and Prospects of Ionic Liquids in Cross-Coupling Reactions. *Top. Curr. Chem.* **2019**, *377*, 1–43. [CrossRef] [PubMed]
51. Yousaf, M.; Zahoor, A.F.; Akhtar, R.; Ahmad, M.; Naheed, S. Development of green methodologies for Heck, Chan–Lam, Stille and Suzuki cross-coupling reactions. *Mol. Divers.* **2019**, *28*, 1–19. [CrossRef] [PubMed]
52. Boruah, P.R.; Gehlot, P.S.; Kumar, A.; Sarma, D. Palladium immobilized on the surface of MMT K 10 with the aid of [BMIM][BF4]: An efficient catalyst for Suzuki-Miyaura cross-coupling reactions. *Mol. Catal.* **2018**, *461*, 54–59. [CrossRef]
53. Hooshmand, S.E.; Heidari, B.; Sedghi, R.; Varma, R.S. Recent advances in the Suzuki-Miyaura cross-coupling reaction using efficient catalysts in eco-friendly media. *Green Chem.* **2019**, *21*, 381–405. [CrossRef]
54. Massaro, M.; Riela, S.; Lazzara, G.; Gruttadauria, M.; Milioto, S.; Noto, R. Green conditions for the Suzuki reaction using microwave irradiation and a new HNT-supported ionic liquid-like phase (HNT-SILLP) catalyst. *Appl. Organomet. Chem.* **2014**, *28*, 234–238. [CrossRef]
55. Kudelko, A.; Wróblowska, M.; Jarosz, T.; Katarzyna, Ł. Synthesis, spectral characteristics and electrochemistry of symmetrically substituted hybrids derived from 2,5-bis(4-bromophenyl)-1,3,4-oxadiazole under Suzuki cross-coupling reaction. *Arkivoc* **2015**, *2015*, 287–302. [CrossRef]
56. Wróblowska, M.; Kudelko, A.; Łapkowski, M. Efficient Synthesis of Conjugated 1,3,4-Thiadiazole Hybrids through Palladium-Catalyzed Cross-Coupling of 2,5-Bis(4-bromophenyl)-1,3,4-thiadiazole with Boronic Acids. *Synlett* **2015**, *26*, 2127–2130. [CrossRef]
57. Wróblowska, M.; Kudelko, A.; Kuźnik, N.; Łaba, K.; Łapkowski, M. Synthesis of Extended 1,3,4-Oxadiazole and 1,3,4-Thiadiazole Derivatives in the Suzuki Cross-coupling Reactions. *J. Heterocycl. Chem.* **2017**, *54*, 1550–1557. [CrossRef]
58. Olesiejuk, M.; Kudelko, A.; Swiatkowski, M.; Kruszynski, R. Synthesis of 4-Alkyl-4H-1,2,4-triazole Derivatives by Suzuki Cross-coupling Reactions and Their Luminescence Properties. *Molecules* **2019**, *24*, 652. [CrossRef] [PubMed]
59. Prince, E. (Ed.) *International Tables for Crystallography, Volume C: Mathematical, Physical and Chemical Tables*; Kluwer Academic Publishers: Dordrecht, The Netherlands, 2004.
60. Jeffrey, G.A.; Saenger, W. *Hydrogen Bonding in Biological Structures*; Springer: New York, NY, USA, 1991.
61. Kruszynski, R.; Sierański, T. Can Stacking Interactions Exist beyond the Commonly Accepted Limits? *Cryst. Growth Des.* **2016**, *16*, 587–595. [CrossRef]
62. Melhuish, W.H. Quantum efficiencies of fluorescence of organic substan ces: Effect of solvent and concentration of the fluorescent solute. *J. Phys. Chem.* **1961**, *65*, 229–235. [CrossRef]
63. Birks, J.B.; Dyson, D.J. The relations between the fluorescence and absorption properties of organic molecules. *Proc. R. Soc. Lond. Ser. A Math. Phys. Sci.* **1963**, *275*, 135–148.
64. Brouwer, A.M. Standards for photoluminescence quantum yield measurements in solution (IUPAC technical report). *Pure Appl. Chem.* **2011**, *83*, 2213–2228. [CrossRef]
65. Shamsipur, M.; Chaichi, M.J. A study of quenching effect of sulfur-containing amino acids l-cysteine and l-methionine on peroxyoxalate chemiluminescence of 7-amino-4-trifluoromethylcumarin. *Spectrochim. Acta Part A Mol. Biomol. Spectrosc.* **2005**, *61*, 1227–1231. [CrossRef]
66. D'Auria, S.; Staiano, M.; Kuznetsova, I.M.; Turoverov, K.K. The Combined Use of Fluorescence Spectroscopy and X-Ray Crystallography Greatly Contributes to Elucidating Structure and Dynamics of Proteins. In *Reviews in Fluorescence*; Geddes, C.D., Lakowicz, J.R., Eds.; Springer: Boston, MA, USA, 2005; pp. 25–61.

67. Kayumova, R.R.; Ostakhov, S.S.; Mamykin, A.V.; Muslukhov, R.R.; Iskhakova, G.F.; Ivanov, S.P.; Meshcheryakova, S.A.; Klen, E.E.; Khaliullin, F.A.; Kazakov, V.P. Structure and luminescence of thietane-containing 1,2,4-triazoles. *Russ. J. Gen. Chem.* **2011**, *81*, 1203–1210. [CrossRef]
68. Liu, K.; Shi, W.; Cheng, P. The coordination chemistry of Zn(II), Cd(II) and Hg(II) complexes with 1,2,4-triazole derivatives. *Dalton Trans.* **2011**, *40*, 8475–8490. [CrossRef]
69. Yunusova, S.N.; Novikov, A.S.; Khoroshilova, O.V.; Kolesnikov, I.E.; Demakova, M.Y.; Bolotin, D.S. Solid-state fluorescent 1,2,4-triazole zinc(II) complexes: Self-organization via bifurcated (N[sbnd]H)2···Cl contacts. *Inorg. Chim. Acta* **2020**, *510*, 119660. [CrossRef]
70. Kędzia, A.; Kudelko, A.; Świątkowski, M.; Kruszyński, R. Microwave-promoted synthesis of highly luminescent s-tetrazine-1,3,4-oxadiazole and s-tetrazine-1,3,4-thiadiazole hybrids. *Dye. Pigment.* **2020**, *172*, 107865. [CrossRef]
71. Meng, S.; Duan, A.; Xue, J.; Zheng, X.; Zhao, Y. UV-Vis, Fluorescence, and Resonance Raman Spectroscopic and Density Functional Theoretical Studies on 3-Amino-1,2,4-triazole: Microsolvation and Solvent-Dependent Nonadiabatic Excited State Decay in Solution. *J. Phys. Chem. A* **2018**, *122*, 8530–8538. [CrossRef] [PubMed]
72. Gusev, A.; Braga, E.; Baluda, Y.; Kiskin, M.; Kryukova, M.; Karaush-Karmazin, N.; Baryshnikov, G.; Kuklin, A.; Minaev, B.; Ågren, H.; et al. Structure and tuneable luminescence in polymeric zinc compounds based on 3-(3-pyridyl)-5-(4-pyridyl)-1,2,4-triazole. *Polyhedron* **2020**, *191*, 114768. [CrossRef]
73. Jin, X.D.; Li, B.; Gao, H.; Zhang, X.; Liu, W.Y. Synthesis, crystal structure, fluorescent property and DFT calculations of a new Zn(II) complex based on 3-(2-pyridyl)-5-(4-pyridyl)-1H-1,2,4-triazole. *Chin. J. Struct. Chem.* **2016**, *35*, 1129–1136. [CrossRef]
74. Yao, Y.G.; Yang, J.X.; Zhang, X.; Qin, Y.Y. N-donor auxiliary ligand influence on the coordination mode variations of v-shaped triazole dicarboxylic acid ligand affording seven new luminescent Zn(II) compounds with variable structural motifs. *Cryst. Growth Des.* **2020**, *20*, 6366–6381. [CrossRef]